

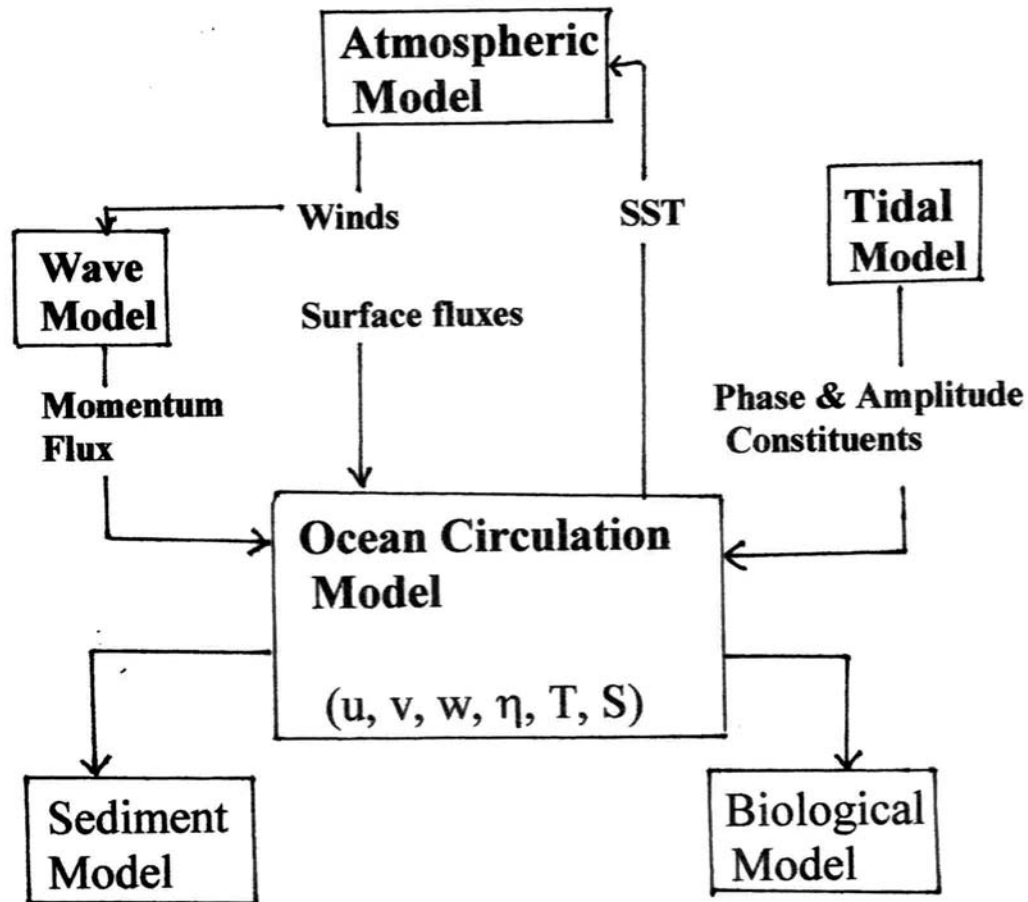
New Development in Coastal Ocean Analysis and Prediction

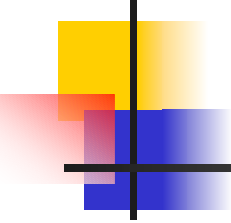
Peter C. Chu

Naval Postgraduate School

Monterey, CA 93943, USA

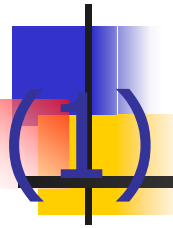
Coastal Model



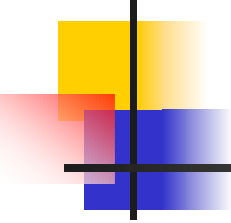


Major Problems in Coastal Modeling

- (1) Discretization
- (2) Sigma Error
- (3) High-Order Scheme
- (4) POM Capability
- (5) Velocity Data Assimilation
- (6) Predictability



(1) Discretization

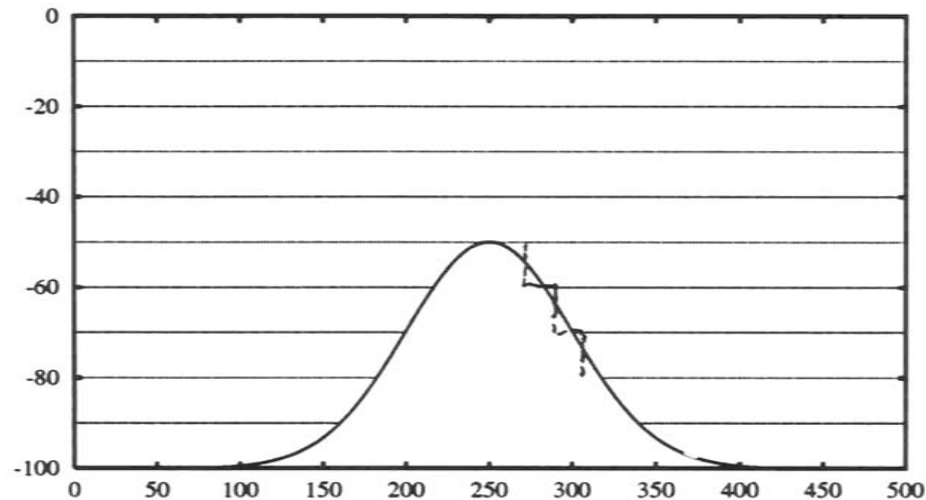


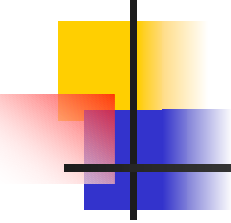
Diversity in Discretization

- Finite Differences
 - Z – coordinate (MOM, ...)
 - σ - coordinate (POM, COHERENS, etc...)
 - s- coordinate (SCRUM, ROMS ...)
 - Layered/Isopycnal coordinates (NLOM, MICOM, ...)
- Finite Elements

Z-Coordiante

- Note "staircase" topography representation, normally with no-slip conditions





Problems of the “Staircase Presentation”

- Difficult in simulating coastal flow.
- Example: Japan/East Sea (JES) Simulation (Kim and Yoon, 1998 JO)

JES Circulation Model Using MOM (Kim & Yoon, 1998)

- 1/6 deg resolution
- 19 vertical level
- Monthly mean wind stress (Na et al. 1992)
- Monthly mean heat flux (Haney type)

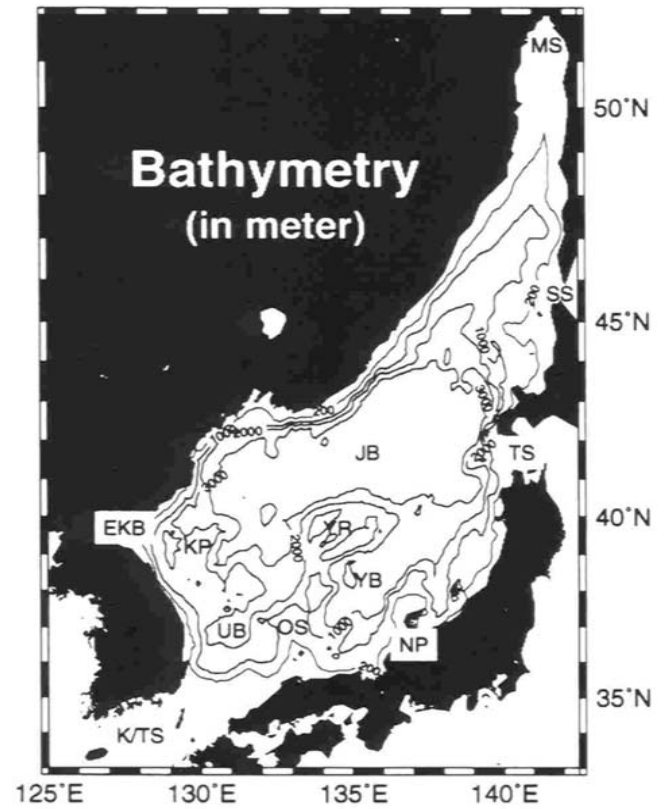
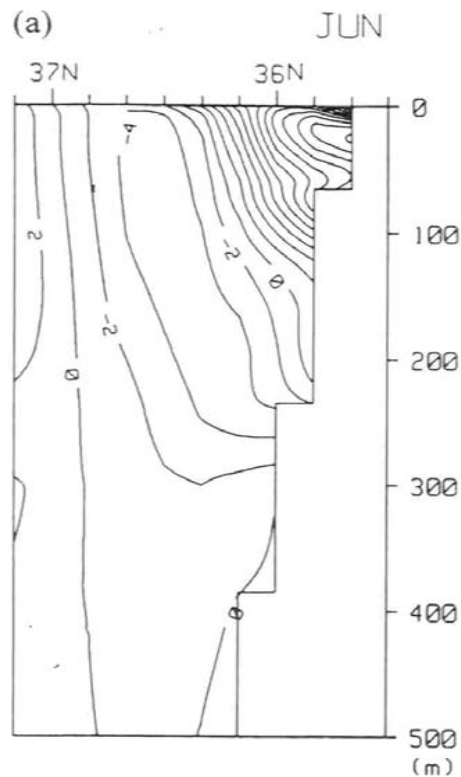


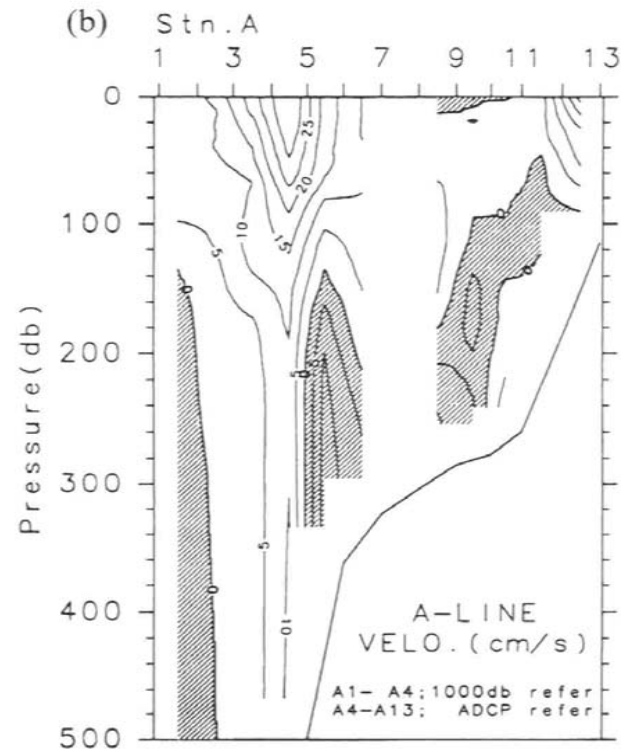
FIG. 1. Bathymetry of the East Sea (125°E-140°E, 35°N-50°N).

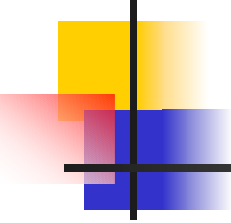
Problem in Simulating Coastal Currents

■ Model



Observation





Layered/Isopycnal Coordinates

■ Pro

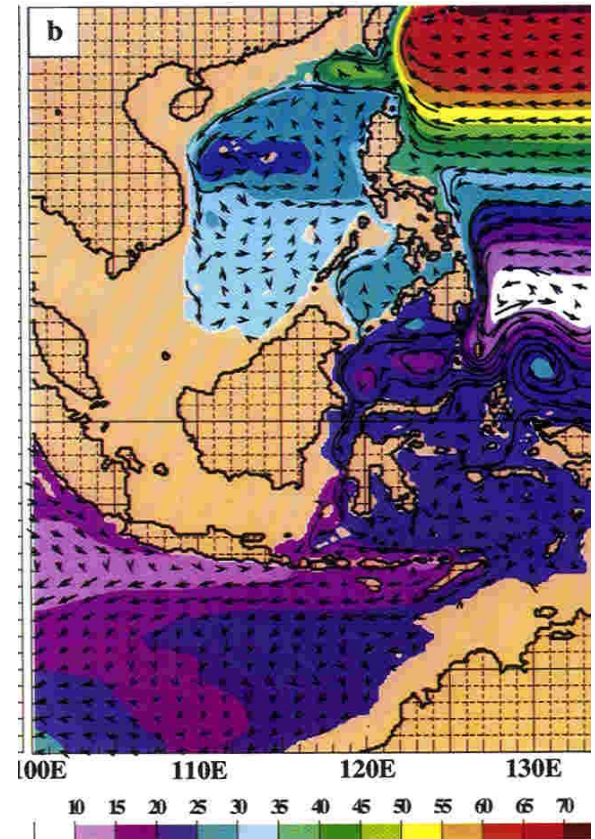
- Horizontal mixing is exactly along the surfaces of constant potential density
- Avoids inconsistencies between vertical and horizontal transport terms

■ Con

- It requires an evident layered structure (not suitable for shelf circulation)
- Some difficulty in modeling detrainment of ocean mixed layer

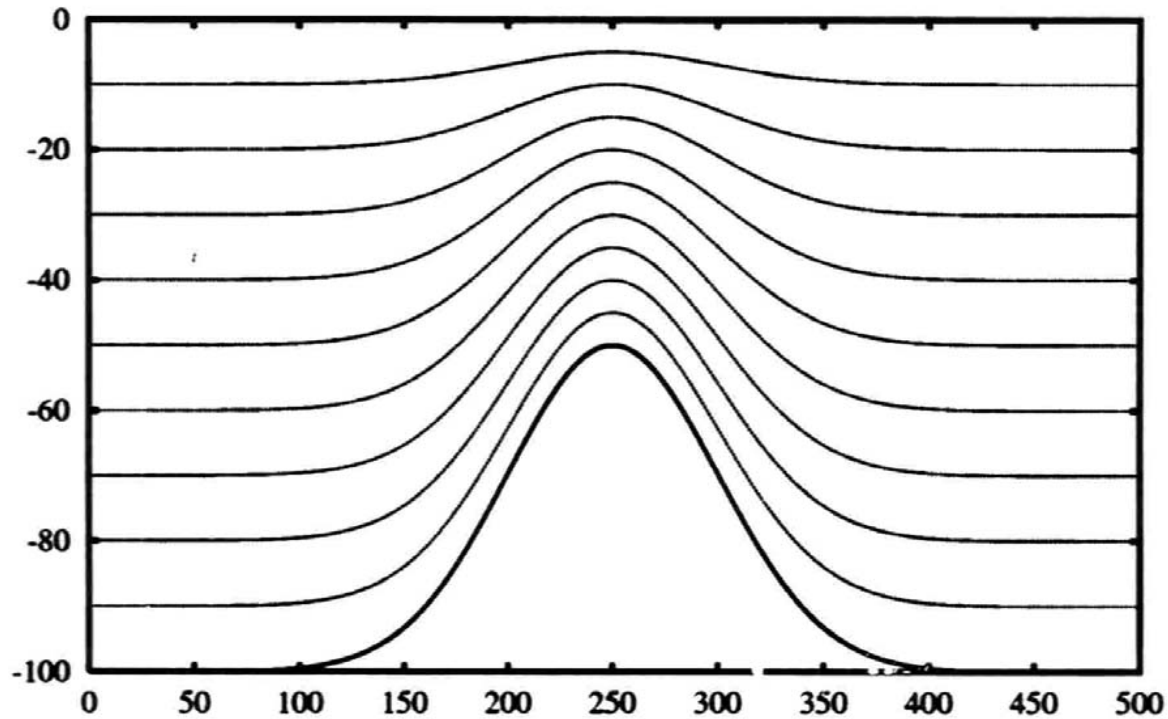
Layered/Isopycnal Coordinates

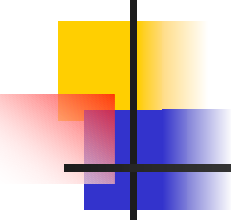
- (Metzger and Hurlburt 1996, JGR)
- $1/8^\circ$, 6 layer with realistic bottom topography
- Not applicable to simulating shelf circulation



Sigma Coordinate Models

Sigma coordinate models





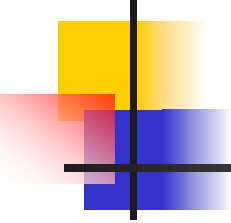
Sigma Coordinates

■ Pro

- Realistic Bottom Topography
- Applicable to Shelf and Estuarine Circulation

■ Con

- Horizontal Pressure gradient Error
- High Vertical Resolution in Shallow Water (Shelf) and Low Resolution in Deep Water



Horizontal Diffusion

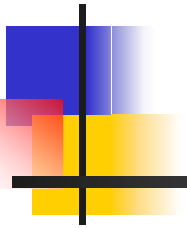
- The second and fourth terms in the righthand side are generally ignored.

Diffusion of tracer fields in Sigma coordinates

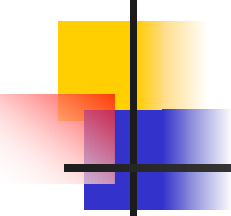
The horizontal mixing becomes

$$\left(\frac{\partial^2 T}{\partial x^2}\right)_z = \left(\frac{\partial^2 T}{\partial x^2}\right)_\sigma + \frac{\partial}{\partial x} \left(\sigma_x \frac{\partial T}{\partial \sigma}\right)_\sigma + \frac{\partial}{\partial \sigma} \left(\sigma_x \frac{\partial T}{\partial x}\right)_\sigma + \sigma_x^2 \frac{\partial^2 T}{\partial \sigma^2},$$

where $\sigma_x = -\frac{\sigma}{h} \frac{\partial h}{\partial x}$.



(2) Sigma Error



Pressure Gradient Error

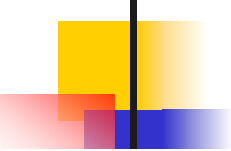
Uses a coordinate system which is scaled with the depth

$$\sigma = \frac{z - \zeta}{H + \zeta}.$$

Makes use of coordinate surfaces which are located below the bottom depth in Level models.

Aspect ratio	Ocean	Atmosphere
$\frac{\Delta h_{\text{topography}}}{H_{\text{depth}}}$	$\sim \mathcal{O}(1)$	$\ll \mathcal{O}(1)$

- **Atmosphere:** Hybrid (σ, p) models are common.
- **Ocean:** ρ and σ surfaces may intersect at large angle.



Pressure Gradient Error

Pressure gradient in Sigma coordinates

$$\frac{\partial P}{\partial x} \Big|_{z=\text{const}} = \frac{\partial P}{\partial x} \Big|_{\sigma=\text{const}} - \frac{\sigma}{h} \frac{\partial h}{\partial x} \frac{\partial P}{\partial \sigma}$$

(1)

Pressure grad
along σ -surfaces

(2)

Correction for
vertical component
in (1)

In case of large slopes:

$$\mathcal{O}(2) = \mathcal{O}(1)$$

$$(1) + (2) \ll (1) \vee (2)$$

Thus, truncation errors may be significant.

Seamount Test Case

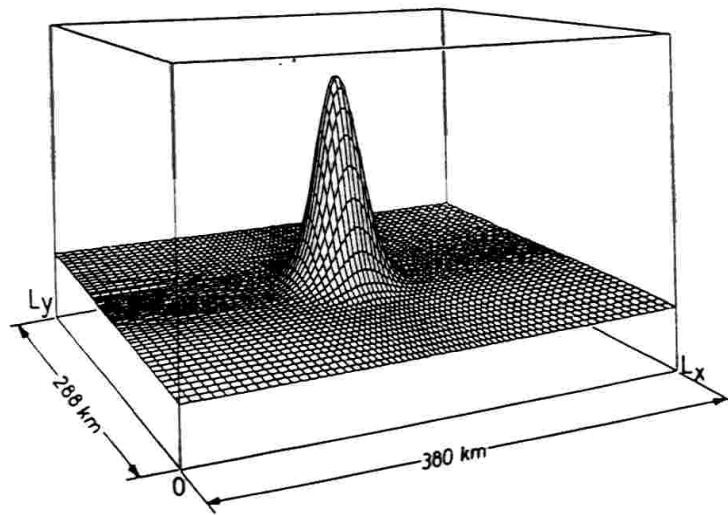


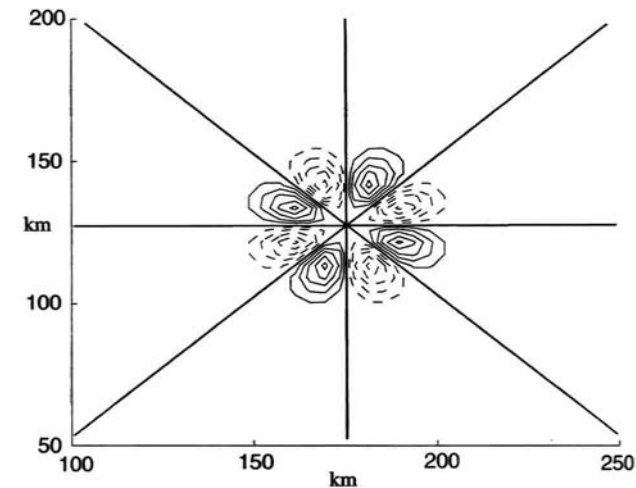
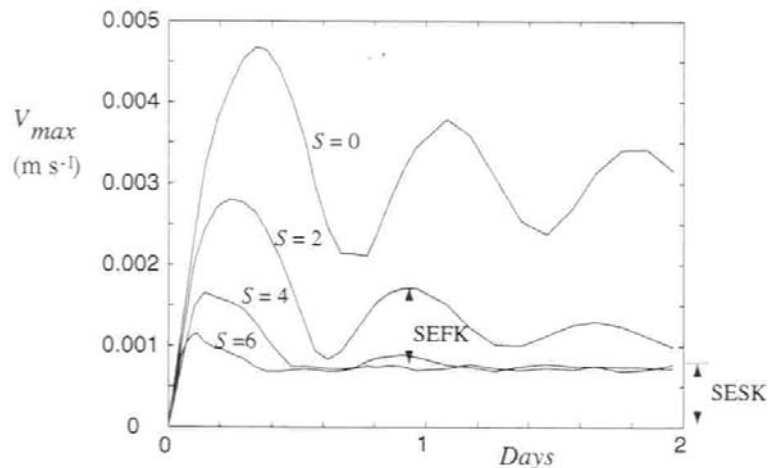
FIG. 1. The seamount geometry. The grid is stretched so that the resolution is highest at the center (after Beckman and Haidvogel 1993).

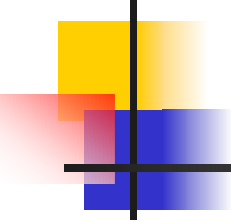
$$S \equiv \frac{N_o H_o}{f_o L} = \frac{(g H_o \Delta_z \rho / \rho_o)^{1/2}}{f_o L},$$

Two Kinds of Sigma Errors (Mellor et al. 1998, JTECH)

- First Kind (SEFK):
Horizontal Density Gradient
Oscillatory Decaying

- Second Kind (SESF)
 - Vorticity Error



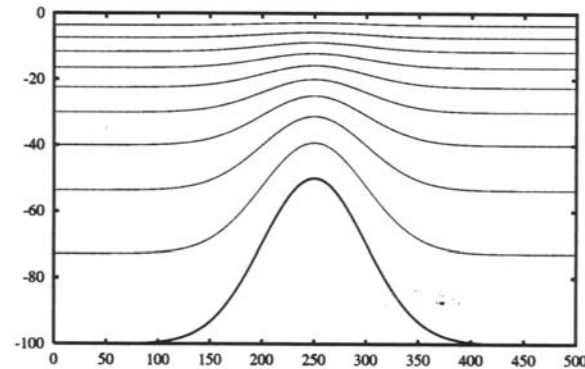


Reduction of Sigma Error

- Smoothing topography
- Subtracting horizontally averaged density field
- Using generalized topography-following coordinate system (e.g., S-coordinates in ROMS)
- Using high-order difference schemes

S-Coordinate Generalized Topography-Following Coordinates (Song & Haidvogel, 1994)

s-coordinate models



Uses a general vertical coordinate scaled with the depth using a nonlinear transformation. More flexible than traditional sigma coordinates (e.g., allows for high resolution in bottom and surface boundary layers).

$$\left. \frac{\partial p}{\partial x} \right)_z = \left. \frac{\partial p}{\partial x} \right)_{z=\zeta} + \frac{g}{\rho_0} \int_s^0 \left\{ \frac{\partial z}{\partial s'} \frac{\partial \rho}{\partial x} - \frac{\partial z}{\partial x} \frac{\partial \rho}{\partial s'} \right\} ds',$$

Error Analysis (S-Coordinate)

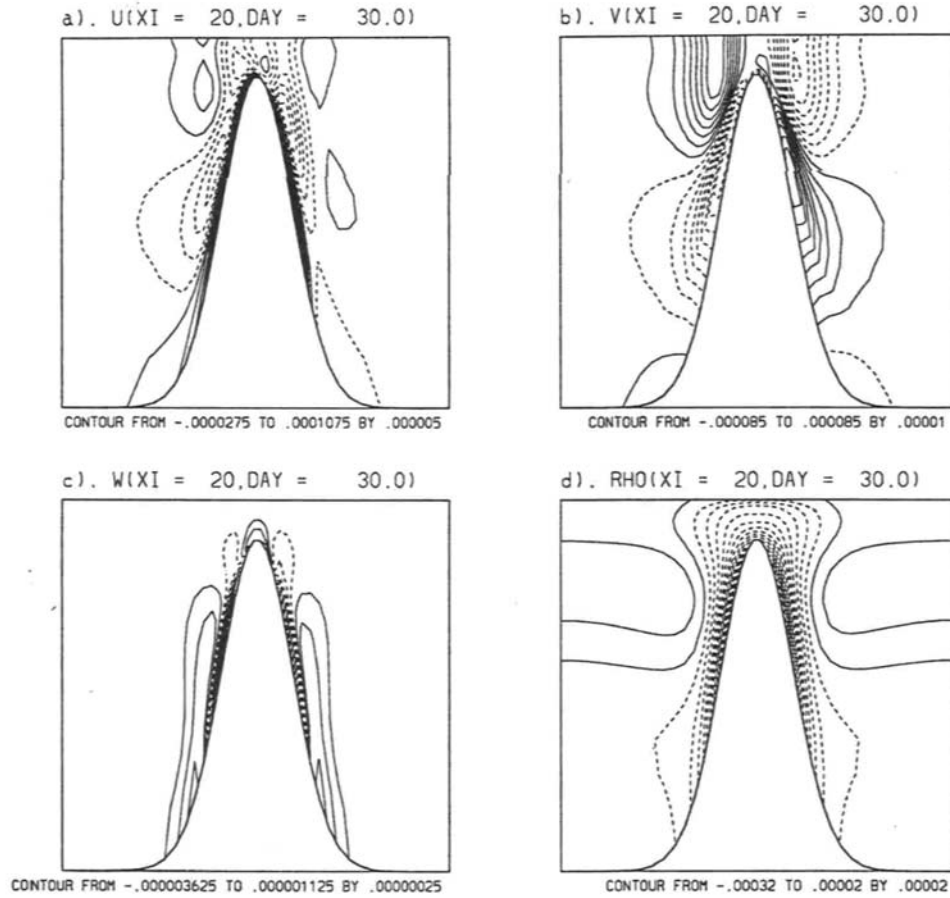
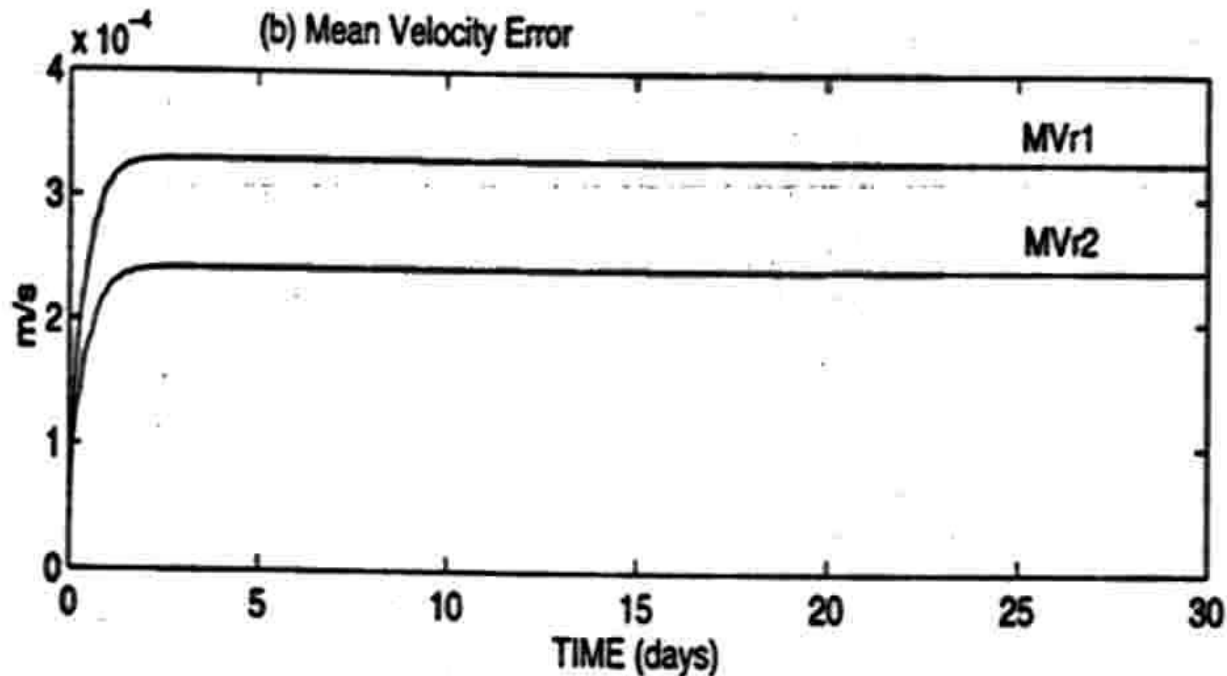
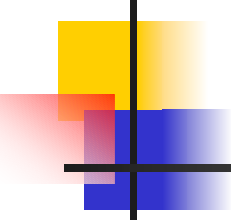


FIG. 1. Cross sections through the center of the seamount: (a) the alongshore velocity; (b) the cross-shore velocity; (c) the vertical velocity; (d) the density change relative to the initial conditions. Units are in m s^{-1} for u , v , w , and in kg m^{-3} for ρ .

Error Evolution (S-coordinate)

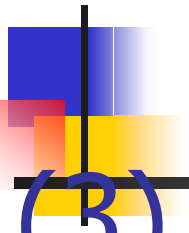
- Radius of Seamount: $r_1 = 40$ km, $r_2 = 80$ km



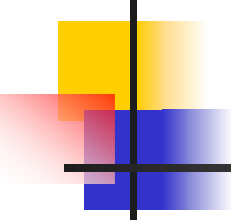


High-Order Schemes

- Ordinary Five-Point Sixth-Order Scheme (Chu and Fan, 1997 JPO)
- Three-Point Sixth-Order Combined Compact Difference (CCD) Scheme (Chu and Fan, 1998 JCP)
- Three-Point Sixth-Order Nonuniform CCD Scheme (Chu and Fan, 1999, JCP)
- Three-Point Sixth-Order Staggered CCD Scheme (Chu and Fan, 2000, Math. & Comp. Modeling)
- Accuracy Progressive Sixth-Order Scheme (Chu and Fan, 2001, JTECH)
- Finite Volume Model (Chu and Fan, 2002)



(3) Difference Schemes



Why do we need high-order schemes?

- (1) Most ocean circulation models are hydrostatic.
- (2) If keeping the same physics, the grid space (Δx) should be larger than certain criterion such that the aspect ratio

$$\delta = H / \Delta x \ll 1$$

A Hidden Problem in Second Order Central Difference Scheme

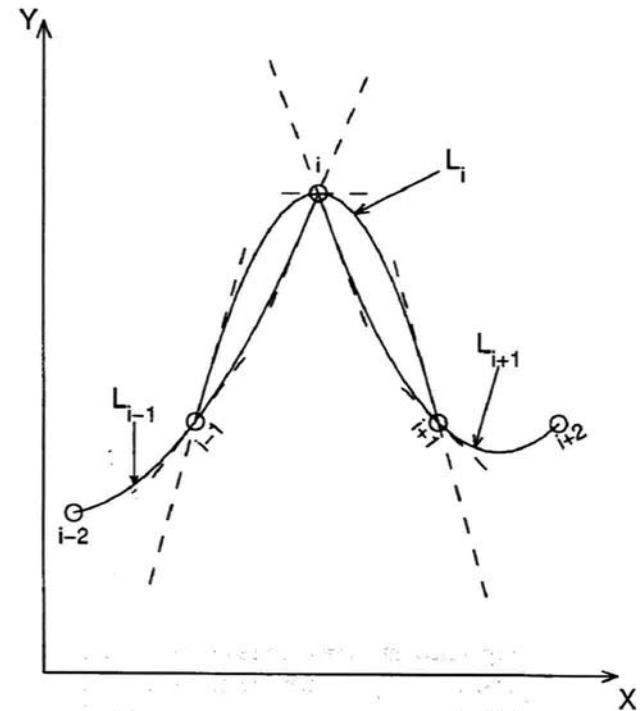
$$\phi'_i = \frac{\phi_{i+1} - \phi_{i-1}}{2\Delta x}$$

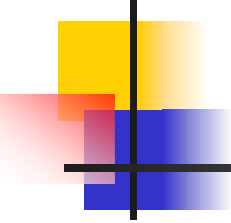
$$\phi''_i = \frac{\phi_{i+1} - 2\phi_i + \phi_{i-1}}{\Delta x^2}$$

- Both Φ' and Φ'' are not continuous at each grid point. This may cause some problems.

Local Hermitian Polynomials

Discontinuity of the first derivatives of the Lagrangian Polynomials at each grid point.



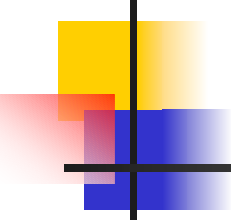


Three-Point Sixth-Order Scheme

$$\begin{aligned} \left(\frac{\delta f}{\delta x}\right)_i + \alpha_1 \left(\left(\frac{\delta f}{\delta x}\right)_{i+1} + \left(\frac{\delta f}{\delta x}\right)_{i-1} \right) + \beta_1 h \left(\left(\frac{\delta^2 f}{\delta x^2}\right)_{i+1} - \left(\frac{\delta^2 f}{\delta x^2}\right)_{i-1} \right) + \dots \\ = \frac{a_1}{2h} (f_{i+1} - f_{i-1}) \end{aligned}$$

$$\begin{aligned} \left(\frac{\delta^2 f}{\delta x^2}\right)_i + \alpha_2 \left(\left(\frac{\delta^2 f}{\delta x^2}\right)_{i+1} + \left(\frac{\delta^2 f}{\delta x^2}\right)_{i-1} \right) + \beta_2 \frac{1}{2h} \left(\left(\frac{\delta f}{\delta x}\right)_{i+1} - \left(\frac{\delta f}{\delta x}\right)_{i-1} \right) + \dots \\ = \frac{a_2}{h^2} (f_{i+1} - 2f_i + f_{i-1}) \end{aligned}$$

.....



Three-Point Sixth Order CCD Schemes

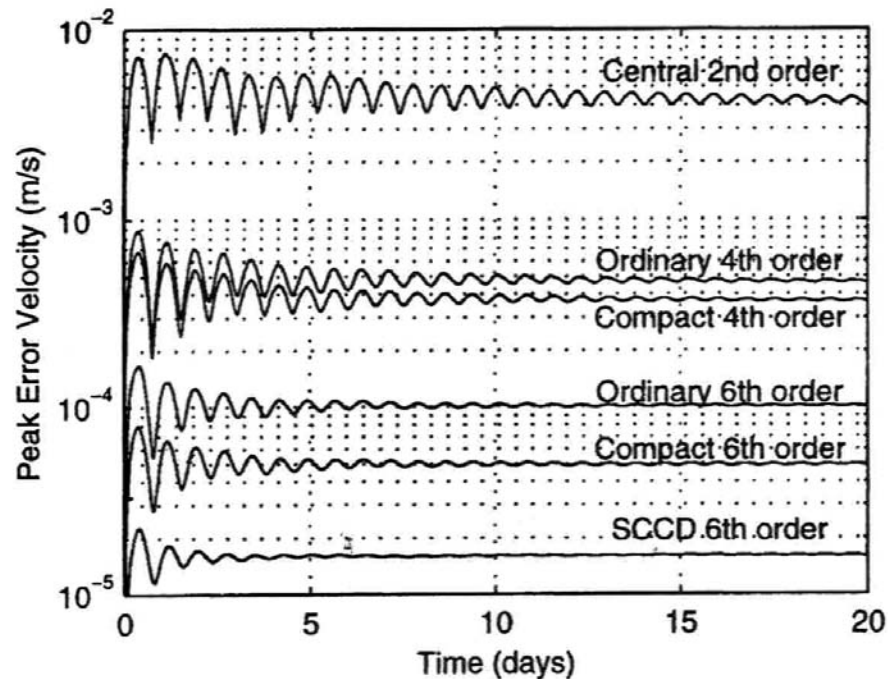
- Existence of Global Hermitian Polynomials
- First Derivative Continuous

$$H'_i(x_i) = H'_{i-1}(x_i) \equiv H'_{i+1}(x_i) = \left(\frac{\delta f}{\delta x} \right)_i$$

- Second Derivative Continuous

$$H''_i(x_i) = H''_{i-1}(x_i) \equiv H''_{i+1}(x_i) = \left(\frac{\delta^2 f}{\delta x^2} \right)_i$$

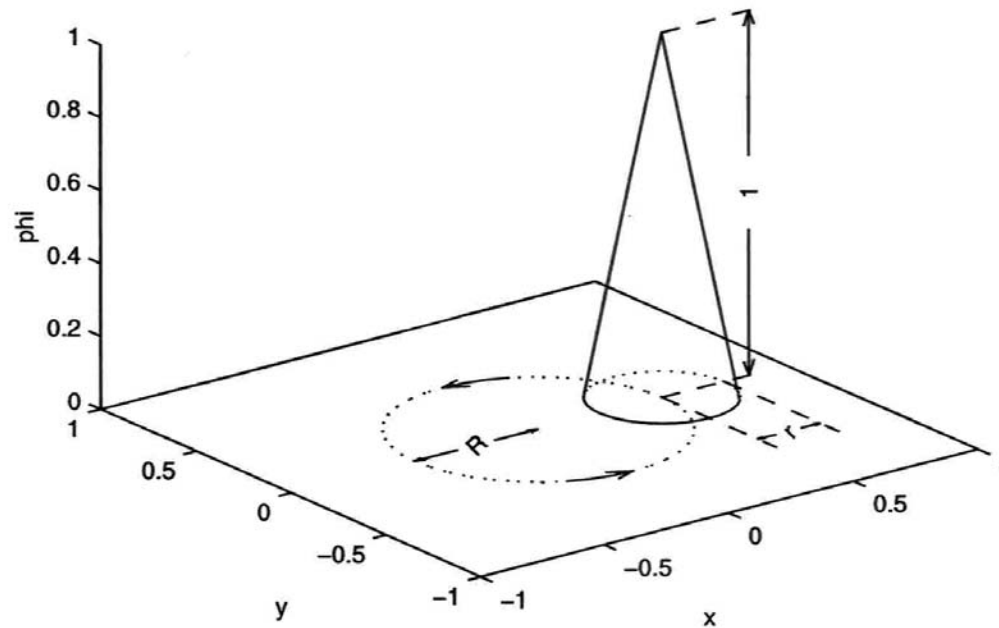
Error Reduction Using CCD Schemes (Seamount)



(a) Peak error velocity.

Figure 11. Peak error velocity propagation in 20 days for the SCCD, second-order, fourth-order, sixth-order ordinary, and sixth-order compact schemes (all staggered). The formulas for the compact schemes compared are listed in the Appendix.

Rotating Cone for Testing Various Schemes



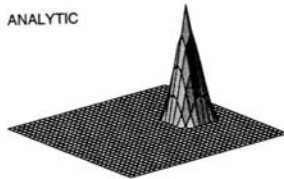
Accuracy Comparison

1 REVOLUTION

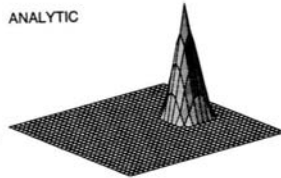
4 REVOLUTIONS

20 REVOLUTIONS

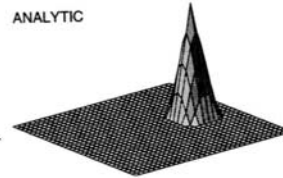
ANALYTIC



ANALYTIC



ANALYTIC



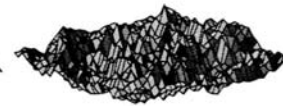
2ND ORDER DIFF



2ND ORDER DIFF



2ND ORDER DIFF



4TH ORDER DIFF



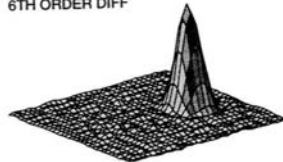
4TH ORDER DIFF



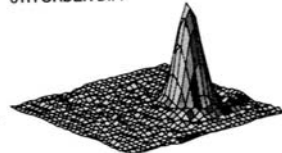
4TH ORDER DIFF



6TH ORDER DIFF



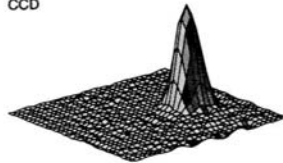
6TH ORDER DIFF



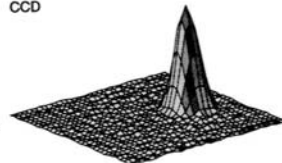
6TH ORDER DIFF



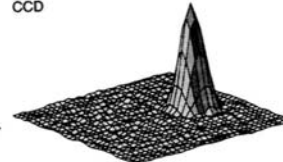
CCD

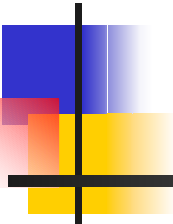


CCD



CCD



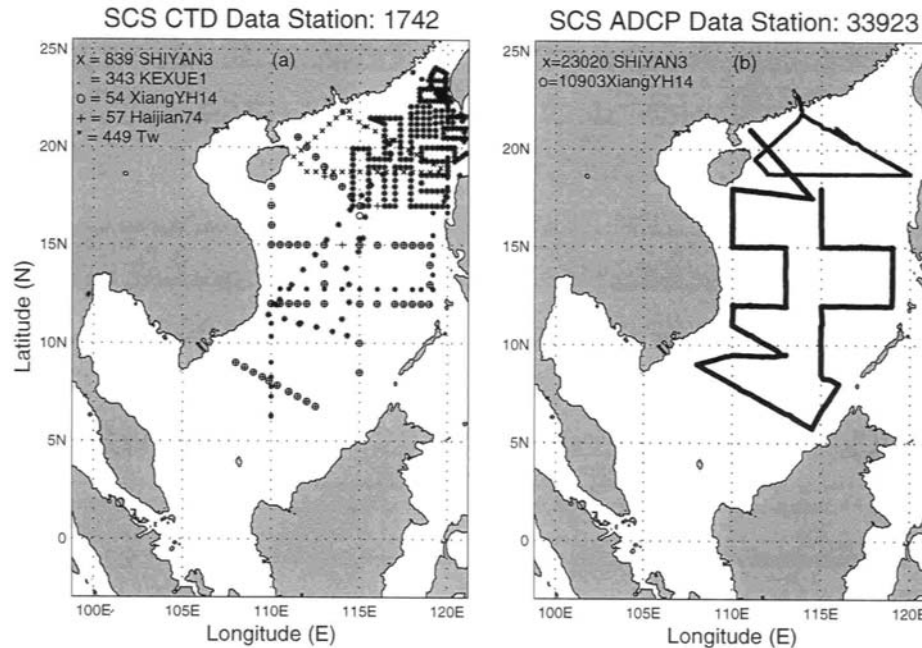


(4) POM Capability

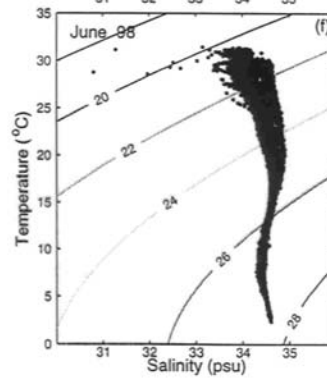
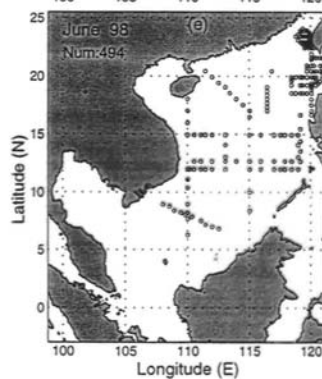
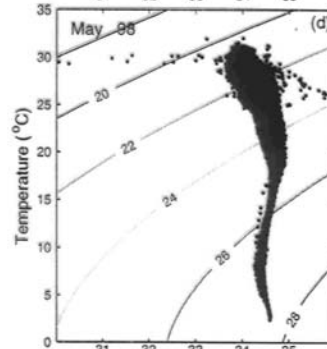
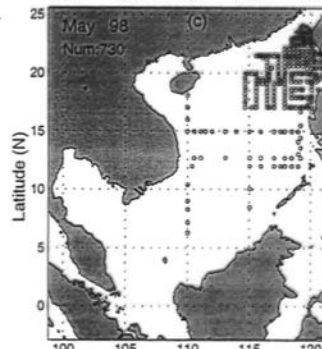
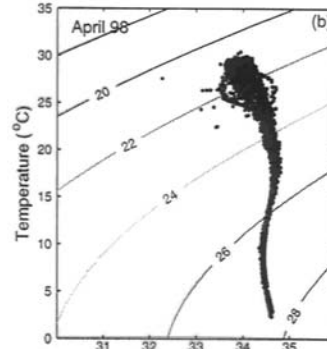
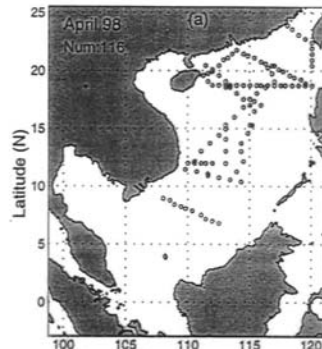
Chu et al 2001, JTECH

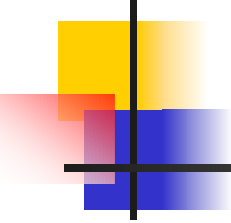
Evaluation of POM Using the South China Sea Monsoon Experiment (SCSMEX) Data

- IOP (April – June 1998)



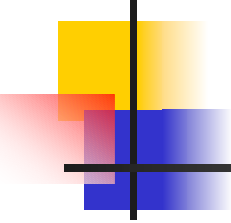
T-S Diagram from SCSMEX Observations





Two Step Initialization of POM

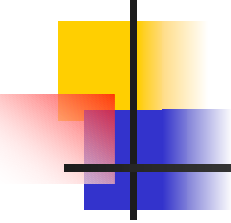
- (1) Spin-up
 - Initial conditions: annual mean (T,S) + zero velocity
 - Climatological annual mean winds + Restoring type thermohaline flux (2 years)
- (2) Climatological Forcing
 - Monthly mean winds + thermohaline fluxes from COADS (3 years) to 1 April
- (3) The final state of the previous step is the initial state of the following step
- (4) Synoptic Forcing
 - NCEP Winds and Fluxes: April 1 to June 30, 1998 (3 Months)



Two Types of Model Integration

- (1) MD1:
 - Without Data Assimilation
 - Hindcast Period: April-June 1998 (3 Months)

- (2) MD2:
 - With Daily SCSMEX-CTD Data Assimilation
 - Hindcast Period:
 - May 1998: No data Assimilation in May
 - June 1998: No data Assimilation in June



Skill-Score

- Model-Data Difference

$$\Delta\psi(x_i, y_j, z, t) = \psi_m(x_i, y_j, z, t) - \psi_o(x_i, y_j, z, t).$$

-
- Mean Square Error

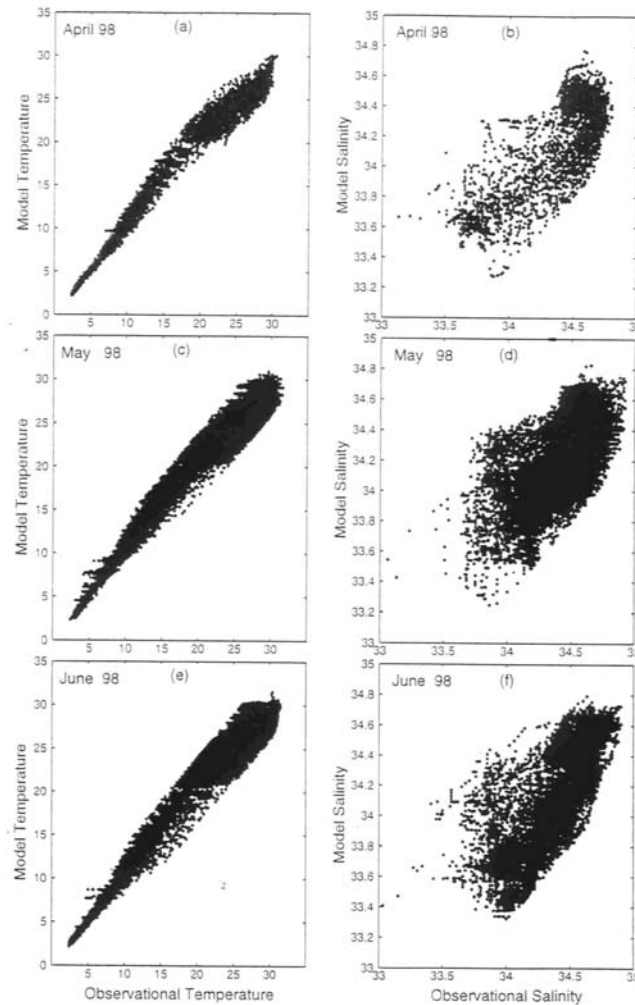
$$\text{MSE}(z, t) = \sum_i \sum_j \frac{1}{N} [\Delta\psi(x_i, y_j, z, t)]^2$$

- Skill-Score (SS)

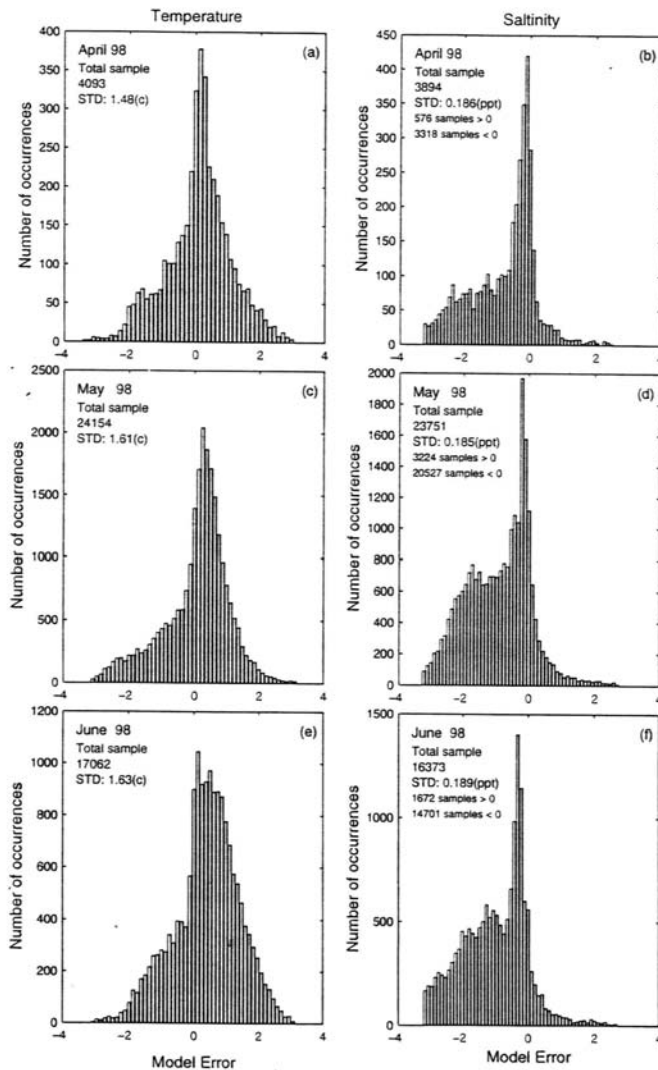
$$SS = 1 - \frac{\text{MSE}(m, o)}{\text{MSE}(c, o)},$$

- $SS > 0$, Model has capability

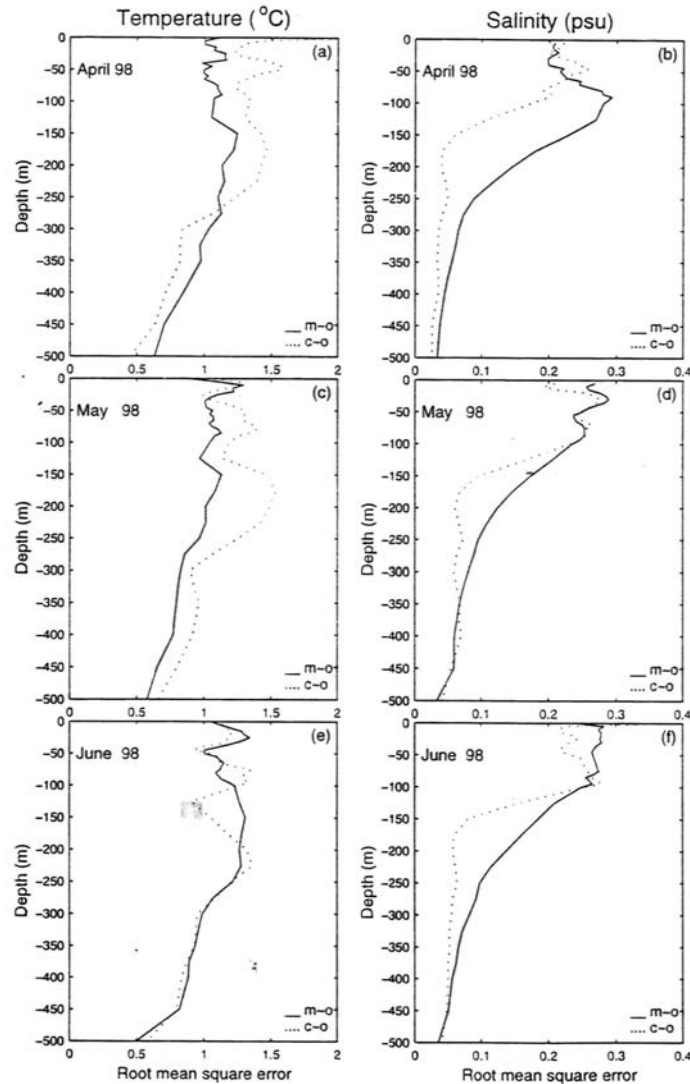
Scatter Diagrams Between Model and Observation (MD1)



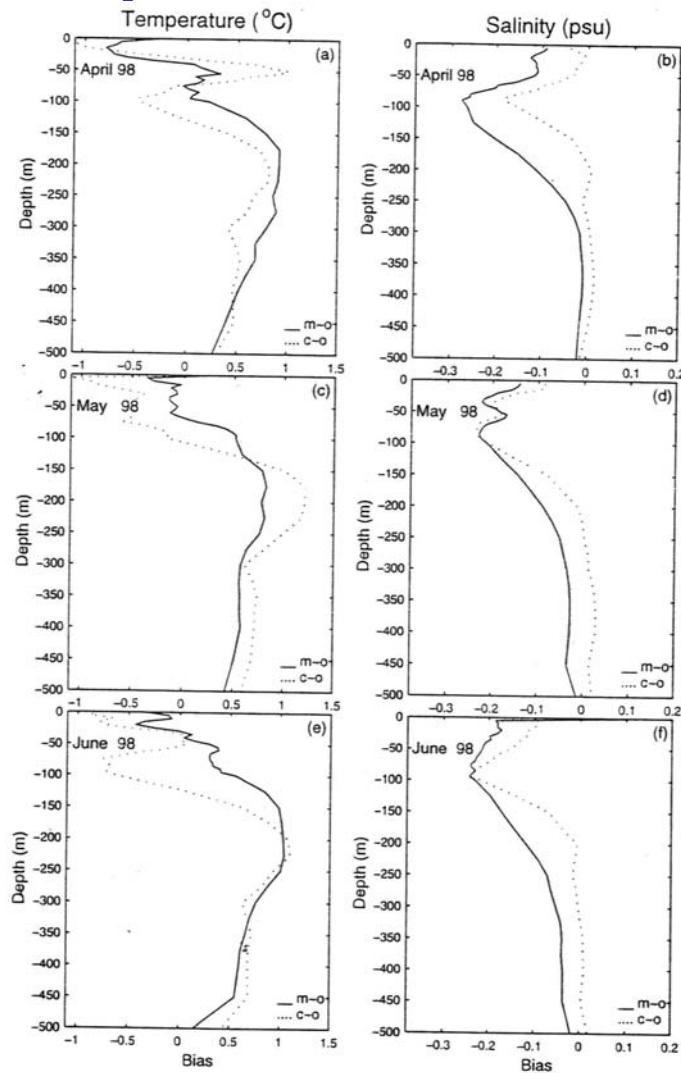
Histograms of (Model – Obs) for MD1



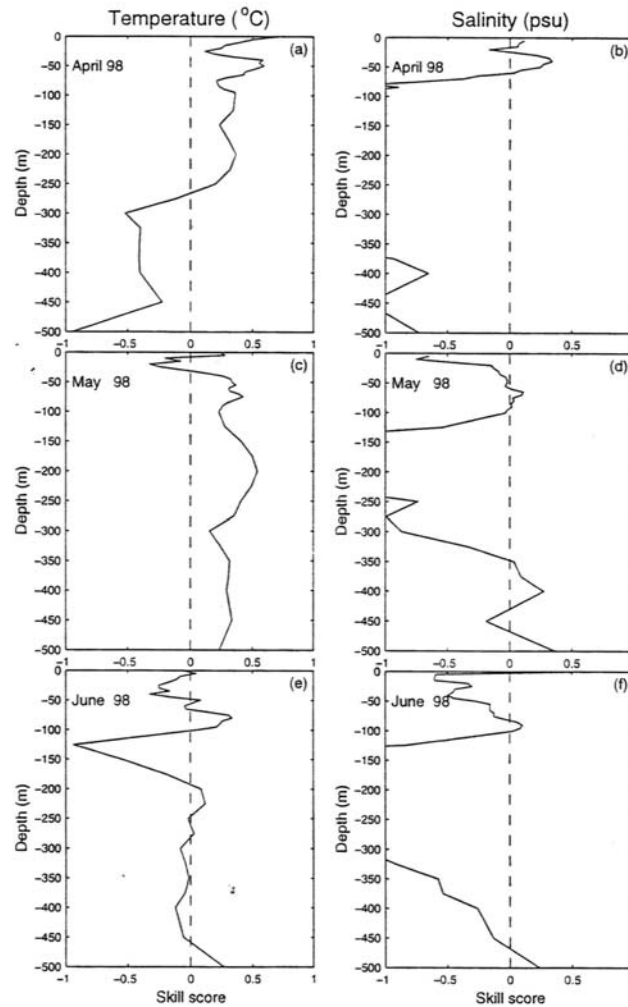
RMS Error for MD1 (No Assimilation)



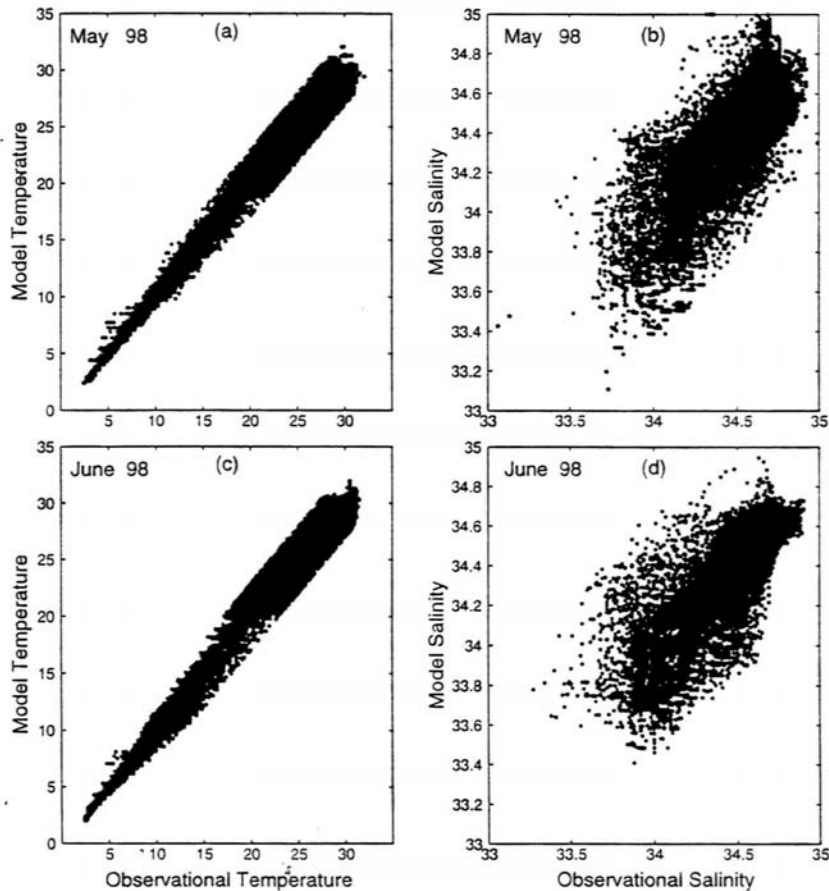
Bias for MD1 (No Assimilation)



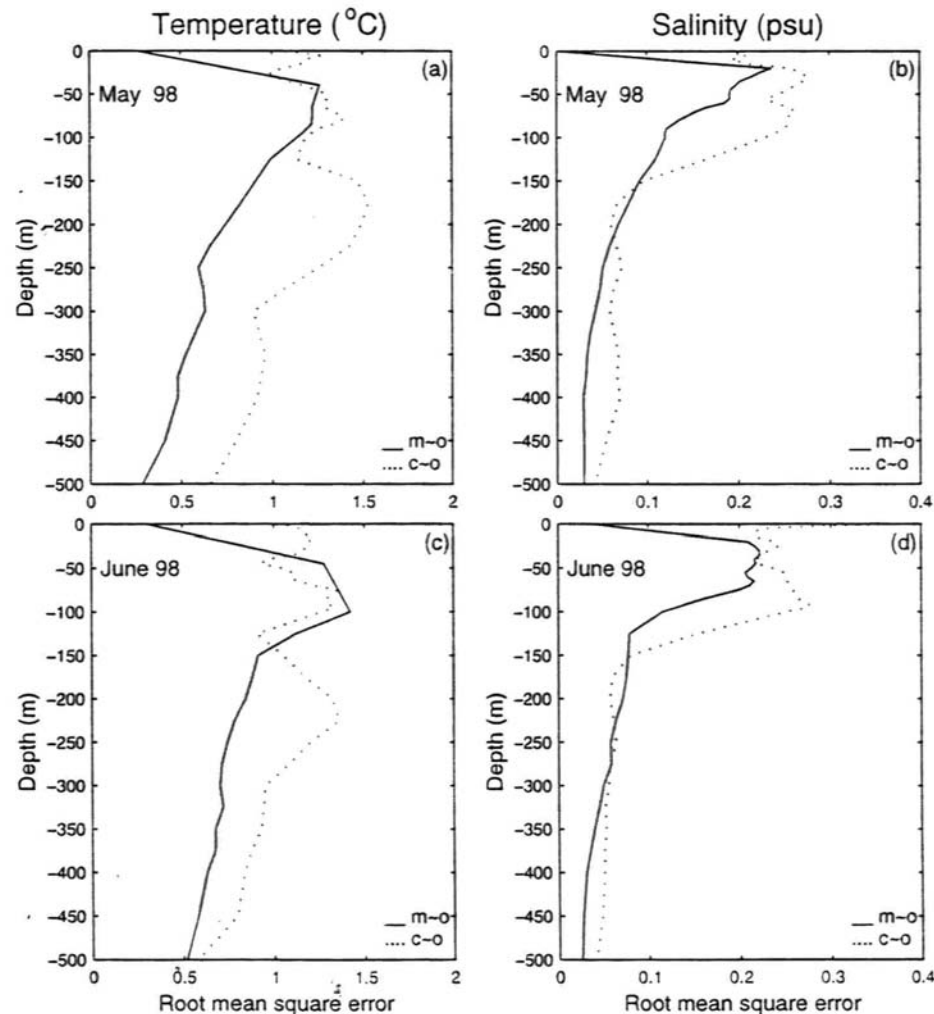
Skill-Score for MD1 (No Assimilation)



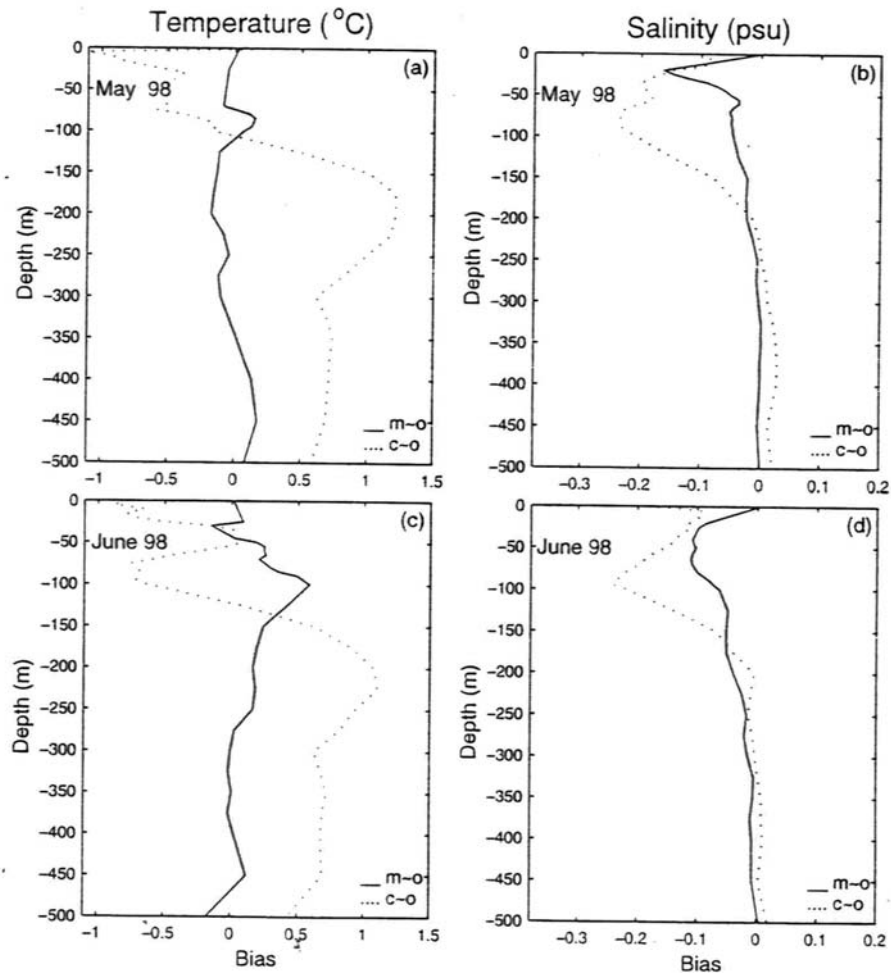
Scatter Diagrams for MD2 (with Assimilation)



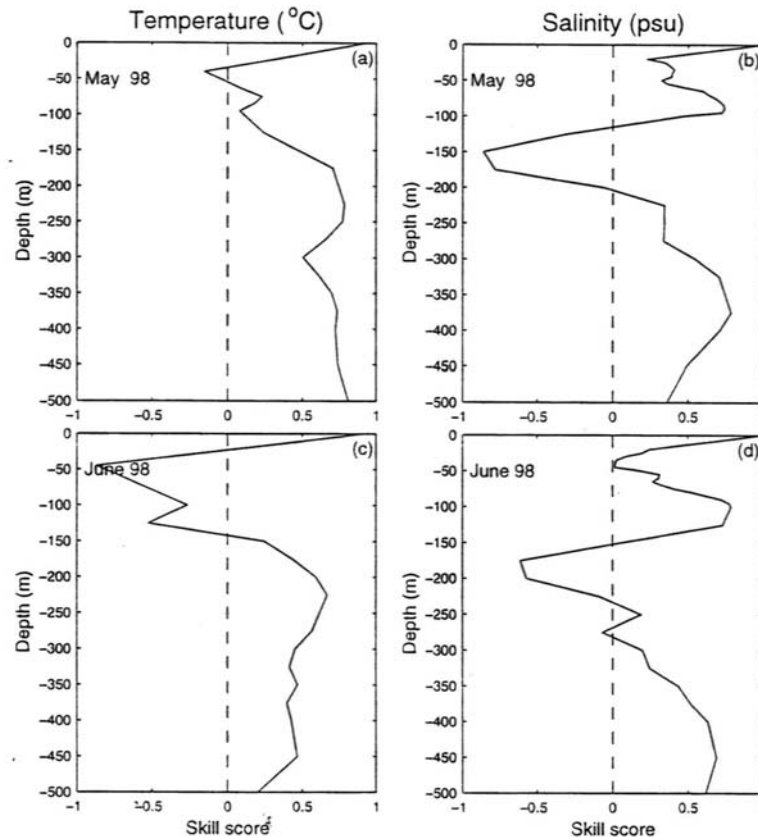
RMS Error for MD2 (with Assimilation)

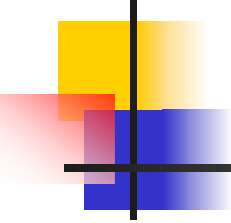


Bias for MD2 (with Assimilation)



Skill-Score for MD2 (with Assimilation)





Comments

- (1) POM-SCS has synoptic flux forcing.
- (2) Without data assimilation, it has capability to predict temperature, but not salinity.
- (3) With data assimilation, it has capability to predict salinity.



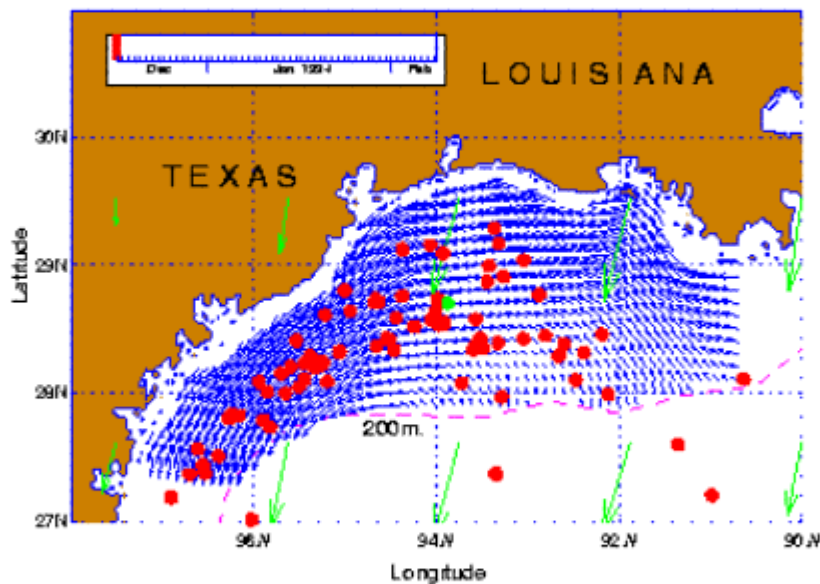
(5) Velocity Data Assimilation

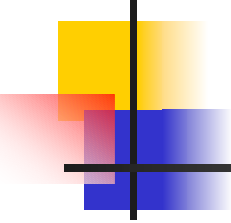
(Chu, et al 2002)



Can we get the velocity field from sparse and noisy data?

Reconstructed Currents from LATEX Drifting Buoy Data (Dec 15, 1993 – Mar 15, 1994)





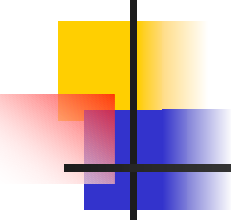
Flow Decomposition

- 2 D Flow (Helmholtz)

$$\mathbf{u}_H = \mathbf{r} \times \nabla_H A_1 + \nabla_H A_3$$

- 3D Flow (Toroidal & Poloidal): Very popular in astrophysics

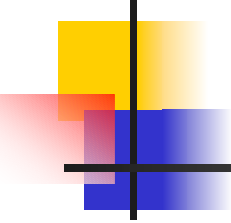
$$\mathbf{u} = \mathbf{r} \times \nabla A_1 + \mathbf{r}A_2 + \nabla A_3$$



3D Incompressible Flow

-
- When $\nabla \cdot \mathbf{u} = 0$
- We have

$$\mathbf{u} = \nabla \times (\mathbf{r}\Psi) + \nabla \times \nabla \times (\mathbf{r}\Phi).$$



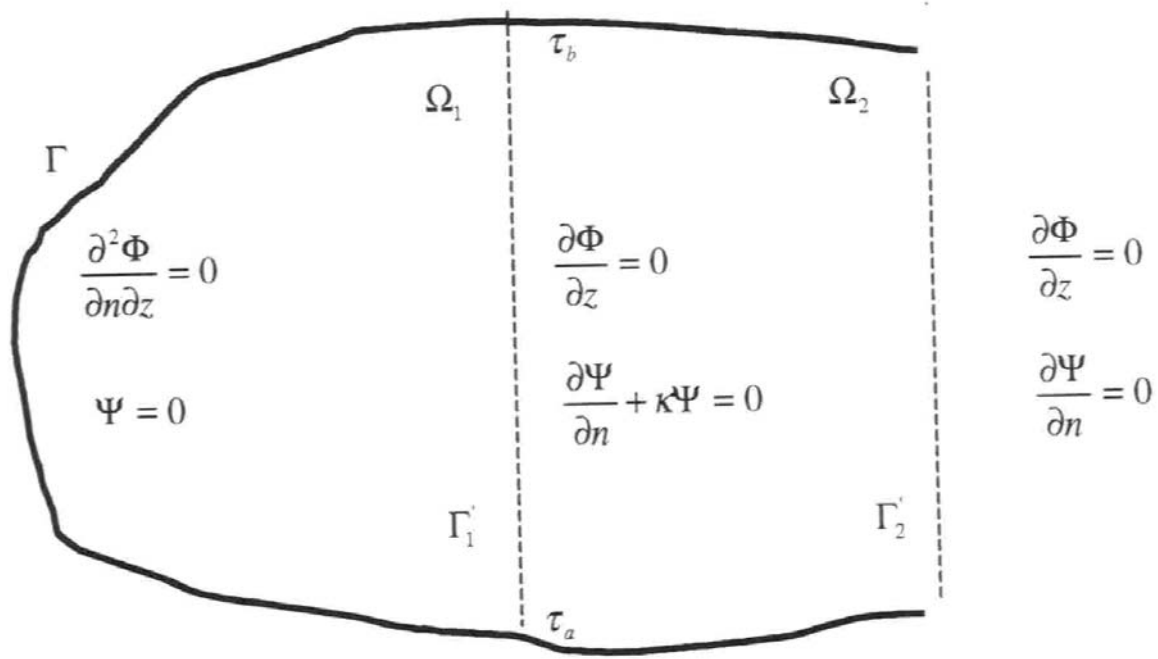
Flow Decomposition

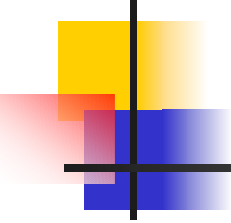
$$u = \frac{\partial \Psi}{\partial y} + \frac{\partial^2 \Phi}{\partial x \partial z}, \quad v = -\frac{\partial \Psi}{\partial x} + \frac{\partial^2 \Phi}{\partial y \partial z},$$

- $\nabla^2 \Psi = -\zeta$, ζ is relative
vorticity

- $\nabla^2 \Phi = -W$

Boundary Conditions

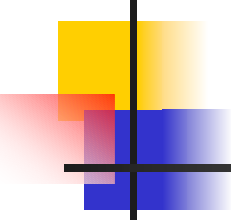




Basis Functions

$$\Psi(x, y, z, t^\circ) = \sum_{k=1}^{\infty} a_k(z, t^\circ) \Psi_k(x, y, z, \kappa^\circ),$$

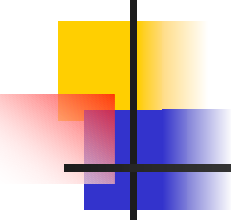
$$\frac{\partial \Phi(x, y, z, t^\circ)}{\partial z} = \sum_{m=1}^{\infty} b_m(z, t^\circ) \Phi_m(x, y, z),$$



Flow Reconstruction

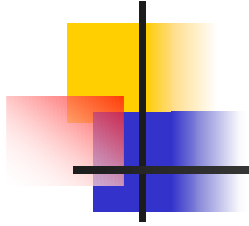
$$u_{KM} = \sum_{k=1}^K a_k(z, t^\circ) \frac{\partial \Psi_k(x, y, z, \kappa^\circ)}{\partial y} + \sum_{m=1}^M b_m(z, t^\circ) \frac{\partial \Phi_m(x, y, z)}{\partial x},$$

$$v_{KM} = - \sum_{k=1}^K a_k(z, t^\circ) \frac{\partial \Psi_k(x, y, z, \kappa^\circ)}{\partial x} + \sum_{m=1}^M b_m(z, t^\circ) \frac{\partial \Phi_m(x, y, z)}{\partial y}$$



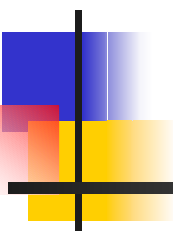
Several Comments

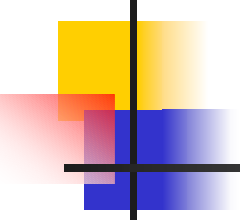
- Reconstruction is a useful tool for processing real-time velocity data with short duration and limited-area sampling.
- The scheme can handle highly noisy data.
- The scheme is model independent.
- The scheme can be used for velocity data assimilation.



6. Predictability

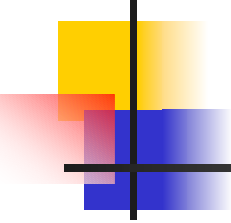
Model Valid Predictability Period (VPP)





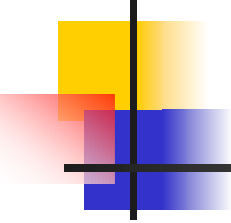
References

- Chu, P.C., L.M. Ivanov, T. M. Margolina, and O.V. Melnichenko, On probabilistic stability of an atmospheric model to various amplitude perturbations. *Journal of the Atmospheric Sciences*, 59, 2860-2873.
- Chu, P.C., L.M. Ivanov, and C.W. Fan, 2002: Backward Fokke-Planck equation for determining model valid prediction period. *Journal of Geophysical Research*, in press.
- Chu, P.C., L.M. Ivanov, L.H. Kantha, O.V. Melnichenko, and Y.A. Poberezhny, 2002: Power law decay in model predictability skill. *Geophysical Research Letters*, in press.



Question

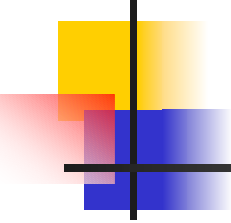
- How long is an ocean (or atmospheric) model valid once being integrated from its initial state?
- Or what is the model valid prediction period (VPP)?



Atmospheric & Oceanic Model (Dynamic System with Stochastic Forcing)

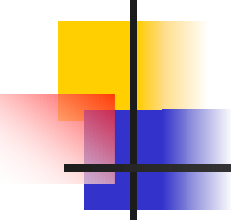


- $d\mathbf{X}/dt = \mathbf{f}(\mathbf{X}, t) + q(t)\mathbf{X}$
- Initial Condition: $\mathbf{X}(t_0) = \mathbf{X}_0$
- Stochastic Forcing:
 - $\langle q(t) \rangle = 0$
 - $\langle q(t)q(t') \rangle = q^2\delta(t-t')$



Prediction Model

- \mathbf{Y} --- Prediction of \mathbf{X}
- Model: $d\mathbf{Y}/dt = \mathbf{h}(\mathbf{y}, t)$
- Initial Condition: $\mathbf{Y}(t_0) = \mathbf{Y}_0$

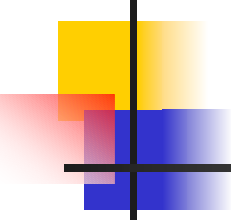


Model Error



$$\mathbf{Z} = \mathbf{X} - \mathbf{Y}$$

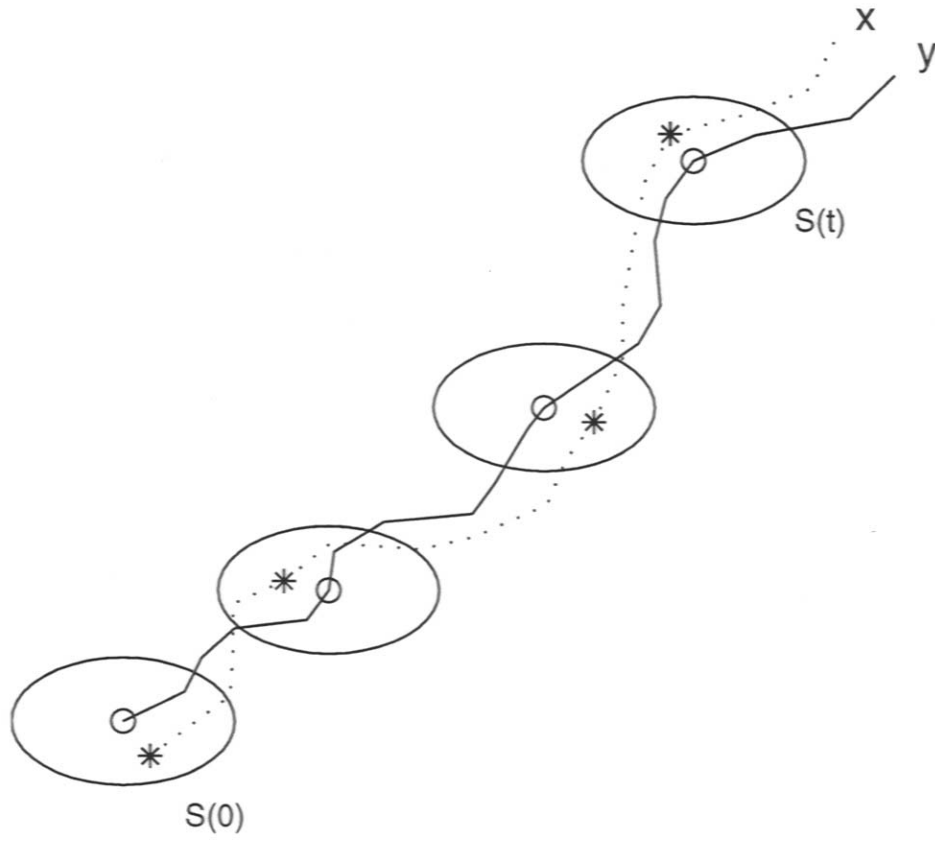
- Initial: $\mathbf{Z}_0 = \mathbf{X}_0 - \mathbf{Y}_0$

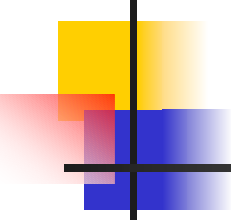


Definition of VPP

- VPP is defined as the time period when the prediction error first exceeds a pre-determined criterion (i.e., the tolerance level ε).

VPP





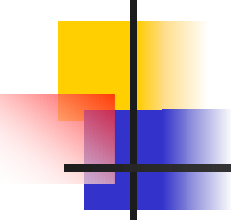
Predictability

- Conventional

- Error Growth
- $\mathbf{Z}(t) = ?$
- For operational model, the vector \mathbf{Z} may have many components

- Using VPP

- One Scalar



Uncertain Initial Error

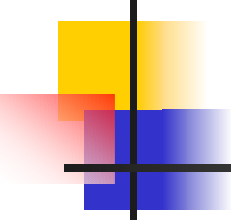
- The prediction is meaningful only if

$$\text{Var}(\mathbf{Z}) \leq \varepsilon^2 \Leftrightarrow \text{ellipsoid } S_\varepsilon(t)$$

-

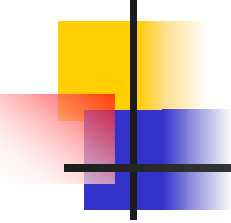
- VPP time period $(t - t_0)$

- Such that $\mathbf{Z} \in S_\varepsilon(t)$



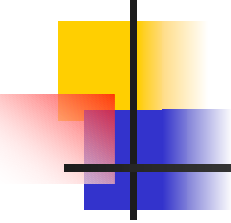
Conditional Probability Density Function

- Initial Error: \mathbf{z}_0
- $(t - t_0)$ Random Variable
- Conditional PDF of $(t - t_0)$ with given \mathbf{z}_0
 - $P[(t - t_0) | \mathbf{z}_0]$
 - Backward Fokker-Planck Equation



Backward Fokker-Planck Equation

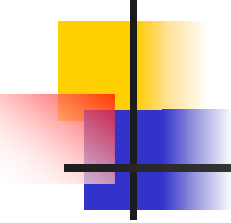
$$\frac{\partial P}{\partial t} - [\mathbf{f}(\mathbf{z}_0, t)] \frac{\partial P}{\partial \mathbf{z}_0} - \frac{1}{2} q^2 \mathbf{z}_0^2 \frac{\partial^2 P}{\partial \mathbf{z}_0 \partial \mathbf{z}_0} = 0$$



Moments

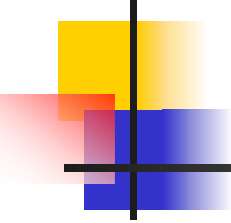
$$\tau_1(\mathbf{z}_0) = \int_{t_0}^{\infty} P(t_0, \mathbf{z}_0, t - t_0)(t - t_0) dt$$

$$\tau_2(\mathbf{z}_0) = \int_{t_0}^{\infty} P(t_0, \mathbf{z}_0, t - t_0)(t - t_0)^2 dt$$



Mean & Variance of VPP

- Mean VPP: τ_1
- Variance of VPP:
 - $\tau_2 - \tau_1^2$

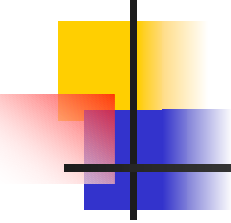


Linear Equations for Mean and Variance of VPP

- For an autonomous dynamical system
- $d\mathbf{X}/dt = \mathbf{f}(\mathbf{X}) + q(t)\mathbf{X}$
- Integration of [Backward F-P Eq. *]
- $(t - t_0), (t - t_0)^2]$ from t_0 to infinity.

$$\mathbf{f}(\mathbf{z}_0) \frac{\partial \tau_1}{\partial \mathbf{z}_0} + \frac{q^2 \mathbf{z}_0^2}{2} \frac{\partial^2 \tau_1}{\partial \mathbf{z}_0 \partial \mathbf{z}_0} = -1$$

$$\mathbf{f}(\mathbf{z}_0) \frac{\partial \tau_2}{\partial \mathbf{z}_0} + \frac{q^2 \mathbf{z}_0^2}{2} \frac{\partial^2 \tau_2}{\partial \mathbf{z}_0 \partial \mathbf{z}_0} = -2\tau_1 .$$



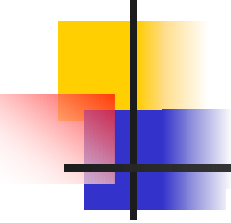
Example 1: One Dimensional Model (Nicolis 1992)

- 1D Dynamical System

$$\frac{d\xi}{dt} = (\sigma - g\xi^2) + v(t)\xi, \quad 0 \leq \xi < \infty$$

$$\langle v(t) \rangle = 0, \quad \langle v(t)v(t') \rangle = q^2 \delta(t-t').$$

$$\sigma = 0.64, \quad g = 0.3, \quad q^2 = 0.2.$$



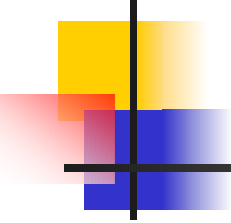
Mean and Variance of VPP

$$(\sigma\xi_0 - g\xi_0^2) \frac{d\tau_1}{d\xi_0} + \frac{q^2\xi_0^2}{2} \frac{d^2\tau_1}{d\xi_0^2} = -1$$

$$(\sigma\xi_0 - g\xi_0^2) \frac{d\tau_2}{d\xi_0} + \frac{q^2\xi_0^2}{2} \frac{d^2\tau_2}{d\xi_0^2} = -2\tau_1$$

$$\tau_1 = 0, \quad \tau_2 = 0 \quad \text{for } \xi_0 = \varepsilon.$$

$$\frac{d\tau_1}{d\xi_0} = 0, \quad \frac{d\tau_2}{d\xi_0} = 0 \quad \text{for } \xi_0 = \xi_{\text{noise}}.$$



Analytical Solutions

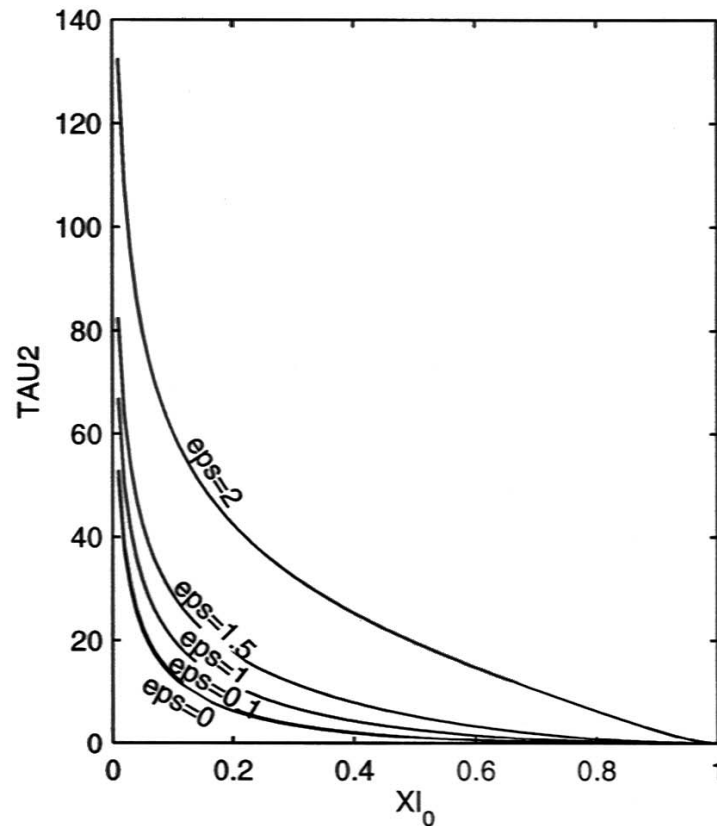
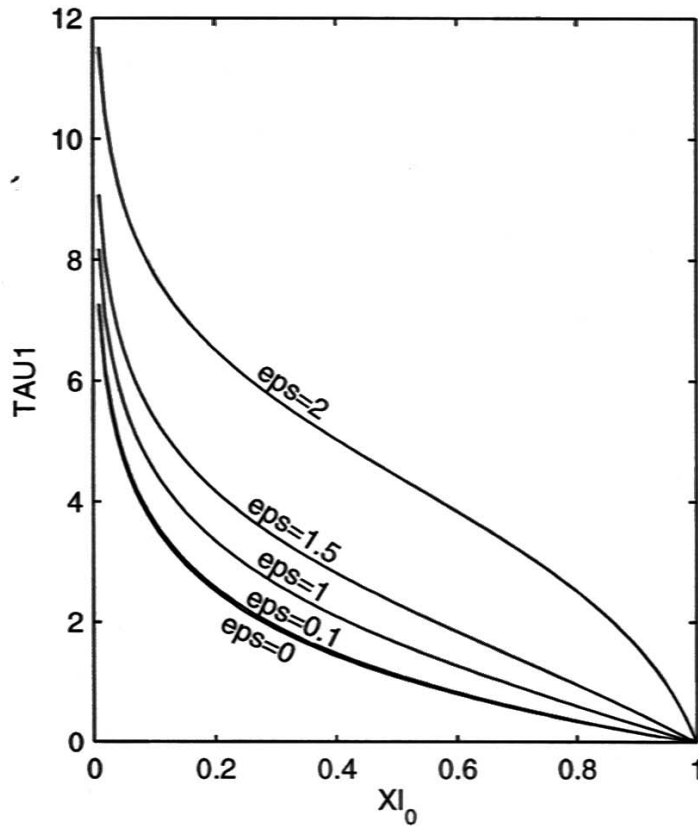
$$\tau_1(\bar{\xi}_0, \bar{\xi}_{noise}, \varepsilon) = \frac{2}{q^2} \int_{\bar{\xi}_0}^1 y^{-\frac{2\sigma}{q^2}} \exp\left(\frac{2\varepsilon g}{q^2} y\right) \left[\int_{\bar{\xi}_{noise}}^y x^{\frac{2\sigma}{q^2}-2} \exp\left(-\frac{2\varepsilon g}{q^2} x\right) dx \right] dy$$

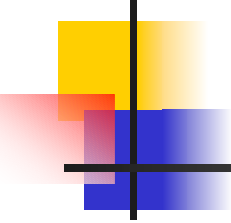
$$\tau_2(\bar{\xi}_0, \bar{\xi}_{noise}, \varepsilon) = \frac{4}{q^2} \int_{\bar{\xi}_0}^1 y^{-\frac{2\sigma}{q^2}} \exp\left(\frac{2\varepsilon g}{q^2} y\right) \left[\int_{\bar{\xi}_{noise}}^y \tau_1(x) x^{\frac{2\sigma}{q^2}-2} \exp\left(-\frac{2\varepsilon g}{q^2} x\right) dx \right] dy$$

$$\bar{\xi}_0 = \xi_0 / \varepsilon,$$

$$\bar{\xi}_{noise} = \xi_{noise} / \varepsilon$$

Dependence of tau1 & tau2 on Initial Condition Error (ξ_0/ε)



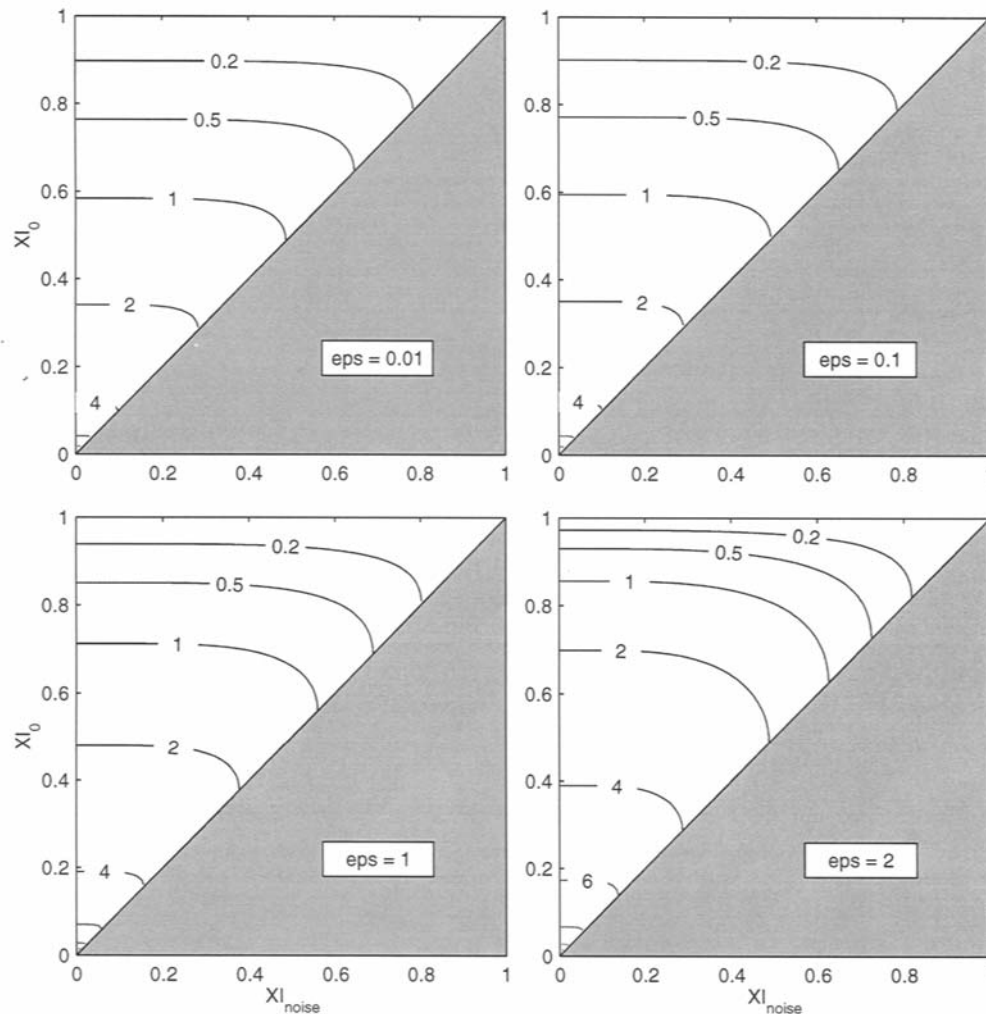


Small Tolerance Error ($\varepsilon \rightarrow 0$)

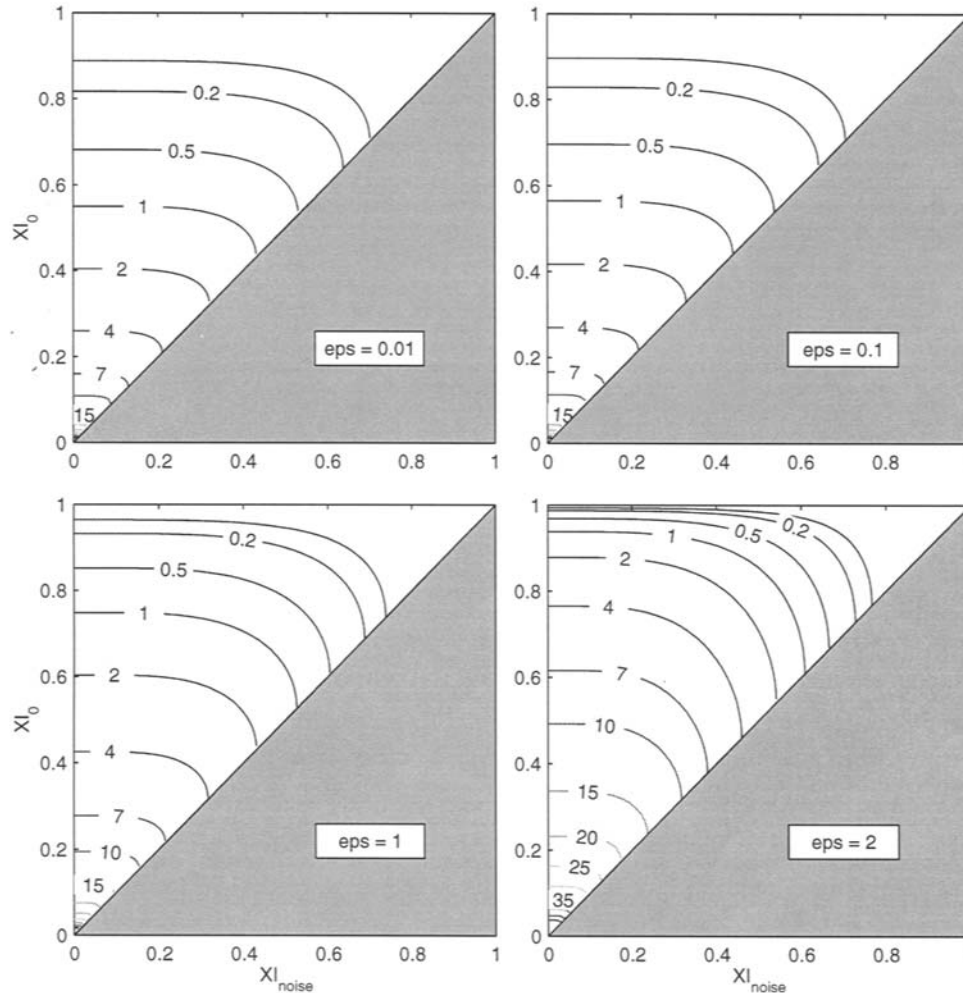
$$\lim_{\varepsilon \rightarrow 0} \tau_1(\bar{\xi}_0, \bar{\xi}_{noise}, \varepsilon) = \frac{1}{\sigma - q^2/2} \left[\ln\left(\frac{1}{\bar{\xi}_0}\right) - \frac{q^2}{2\sigma - q^2} \left(\frac{\bar{\xi}_{noise}}{\bar{\xi}_0}\right)^{\frac{2\sigma}{q^2} - 1} + \frac{q^2}{2\sigma - q^2} \bar{\xi}_{noise}^{\frac{2\sigma}{q^2} - 1} \right]$$

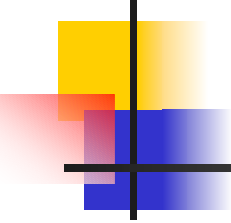
- (1) Lyapunov Exponent: ($\sigma - q^2/2$)
- (2) Stochastic Forcing ($q \neq 0$):
 - Multiplicative White Noise
 - Reducing the Lyapunov exponent (Stabilizing the dynamical system)

Dependence of Mean VPP on initial error and tolerance level

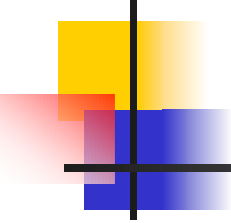


Dependence of Variance of VPP on initial error and tolerance level





Example 2: Multi-Dimensional Models: Power Decay Law in VPP

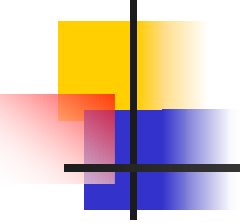


Model Error



$$\mathbf{Z} = \mathbf{X} - \mathbf{Y}$$

- Initial: $\mathbf{Z}_0 = \mathbf{X}_0 - \mathbf{Y}_0$



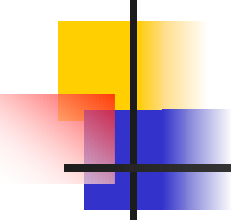
Error Mean and Variance

Error Mean

$$L_1 = \langle \mathbf{z} \rangle$$

Error Variance

$$L_2 = \langle (\mathbf{z} - \langle \mathbf{z} \rangle)^t (\mathbf{z} - \langle \mathbf{z} \rangle) \rangle$$

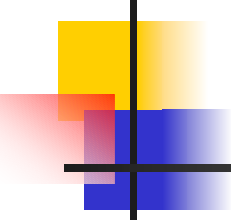


Exponential Error Growth

$$L_1 \propto e^{\sigma t}, \quad L_2 \propto e^{\omega t},$$

Classical Linear Theory

No Long-Term Predictability

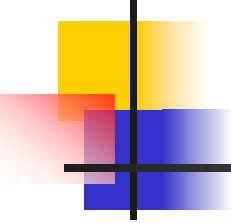


Power Law

$$L_1 \propto t^\alpha, \quad L_2 \propto t^\beta,$$

$$P(t_0, \mathbf{z}_0, \varepsilon, t - t_0) \sim t^{-\gamma} \quad \text{for large } t.$$

Long-Term Predictability May Occur

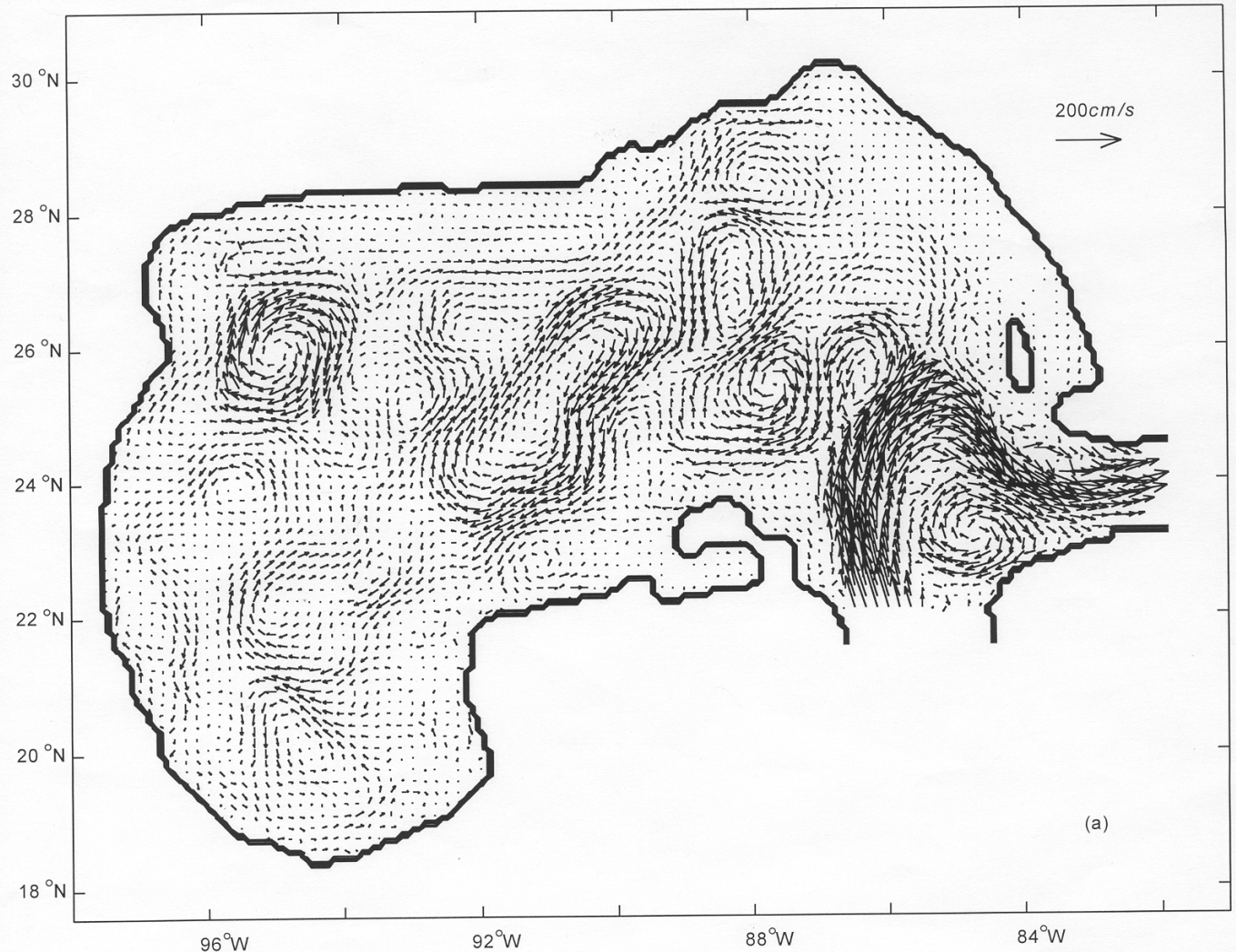


Gulf of Mexico

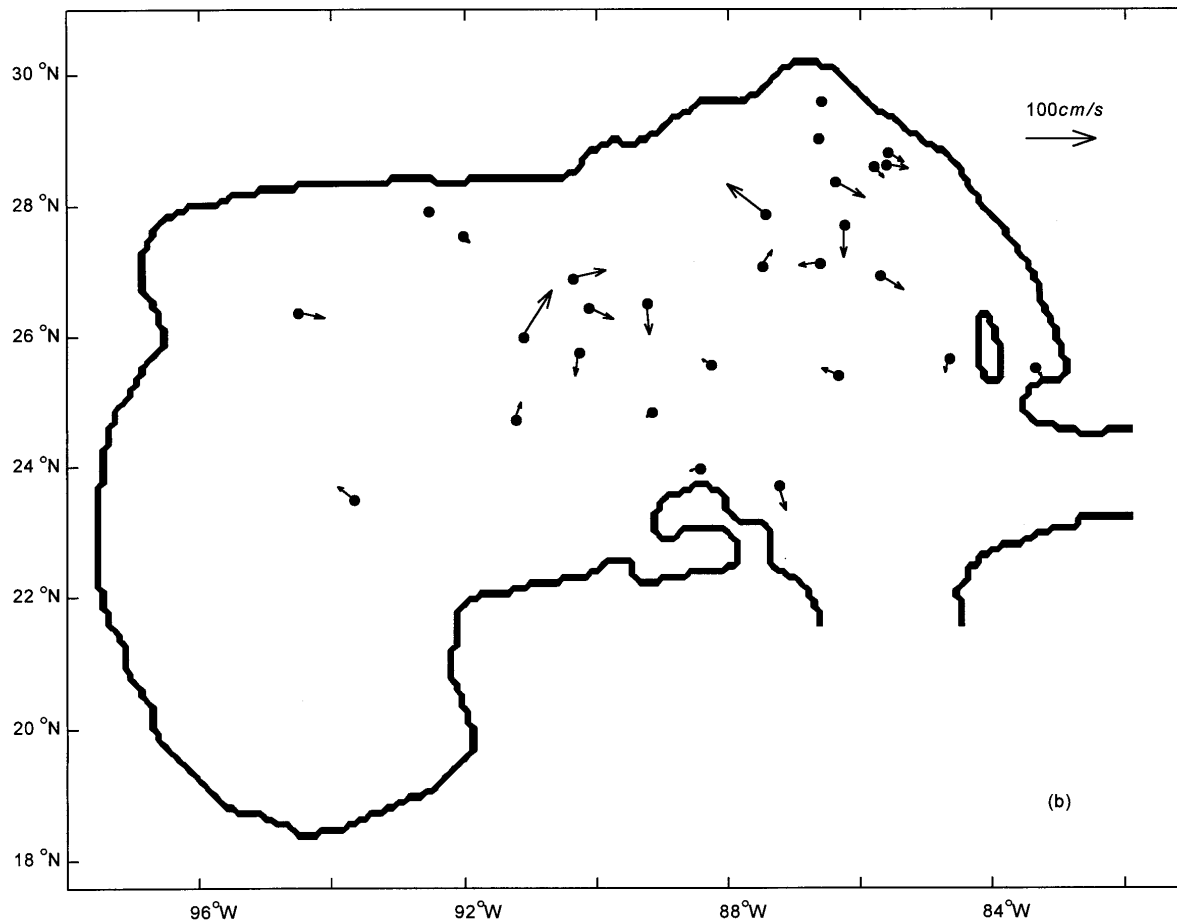
Nowcast/Forecast System

- University of Colorado Version of POM
- $1/12^\circ$ Resolution
- Real-Time SSH Data (TOPEX, ESA ERS-1/2) Assimilated
- Real Time SST Data (MCSST, NOAA AVHRR) Assimilated
- Six Months Four-Times Daily Data From July 9, 1998 for Verification

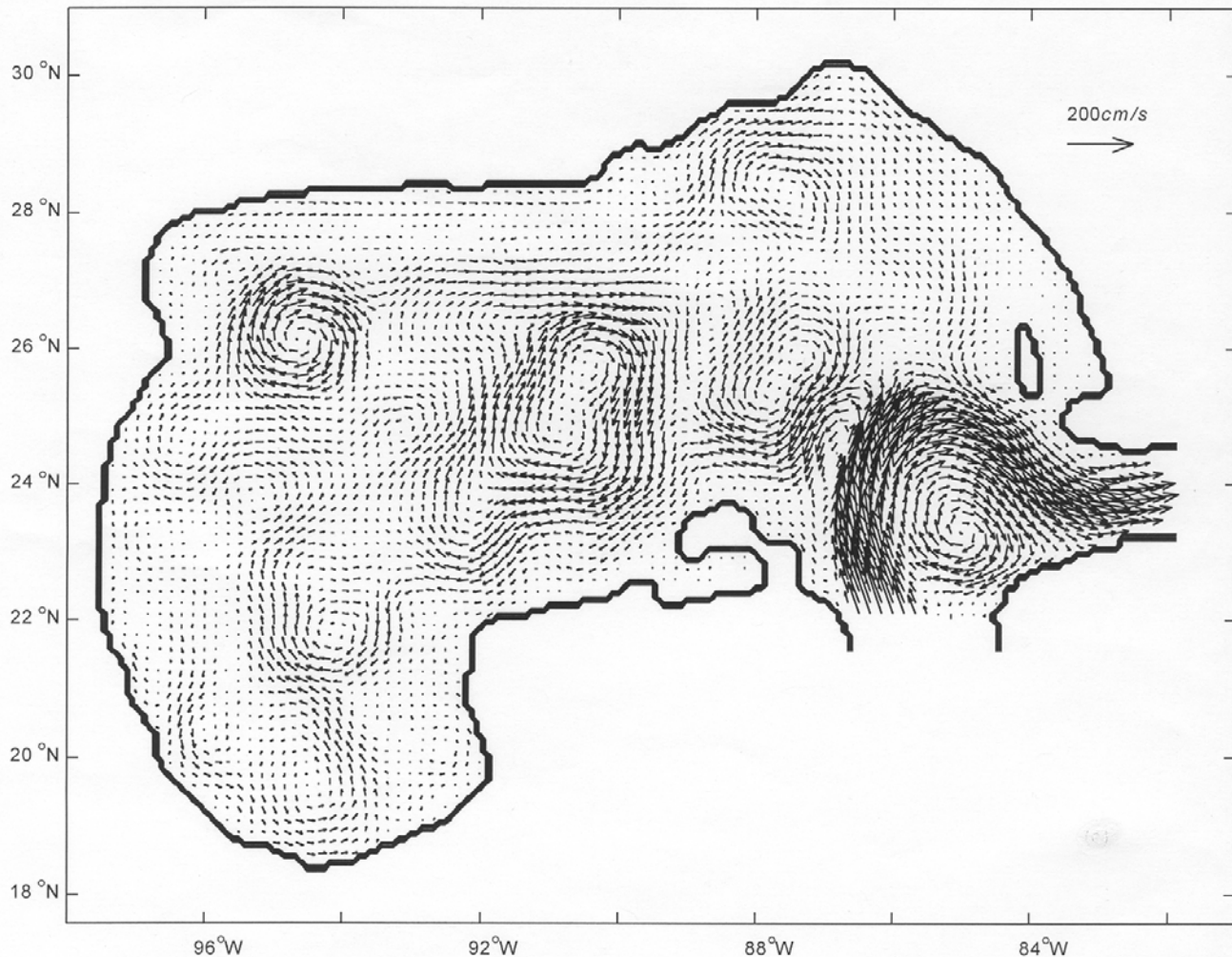
Model Generated Velocity Vectors at 50 m on 00:00 July 9, 1998



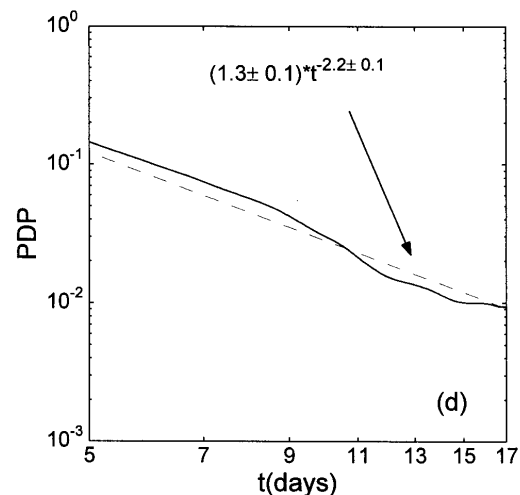
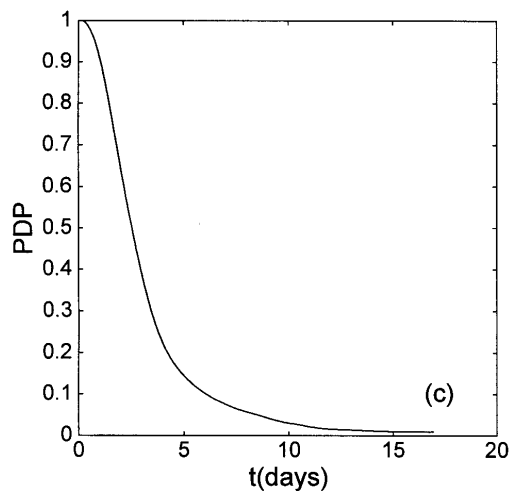
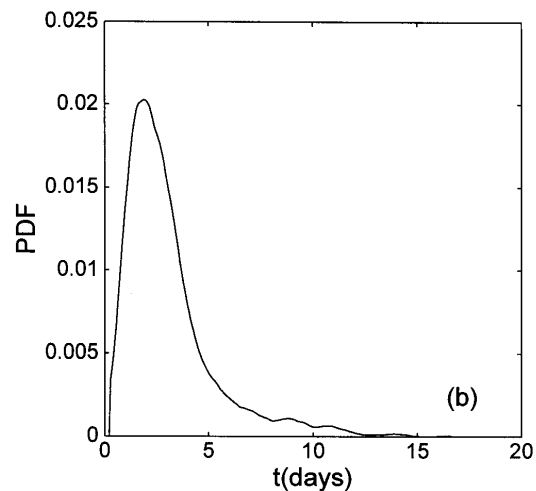
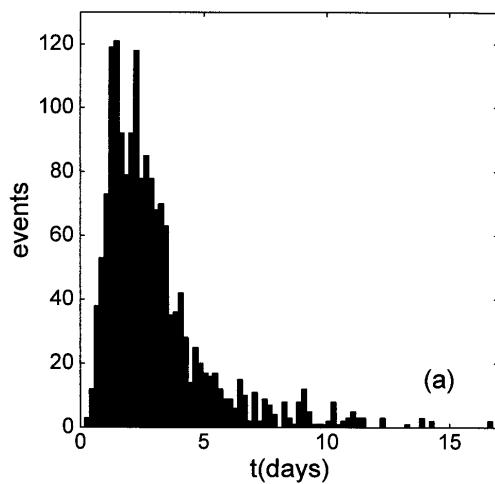
(Observational) Drifter Data at 50 m on 00:00 July 9, 1998

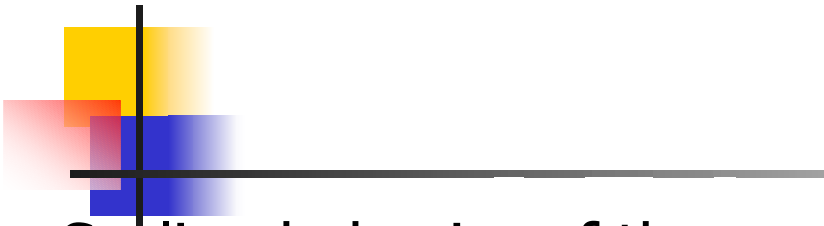


Reconstructed Drift Data at 50 m on 00:00 July 9, 1998 (Chu et al. 2002 a, b, JTECH)



Statistical Characteristics of VPP for zero initial error and 55 km tolerance level (Non-Gaussian)



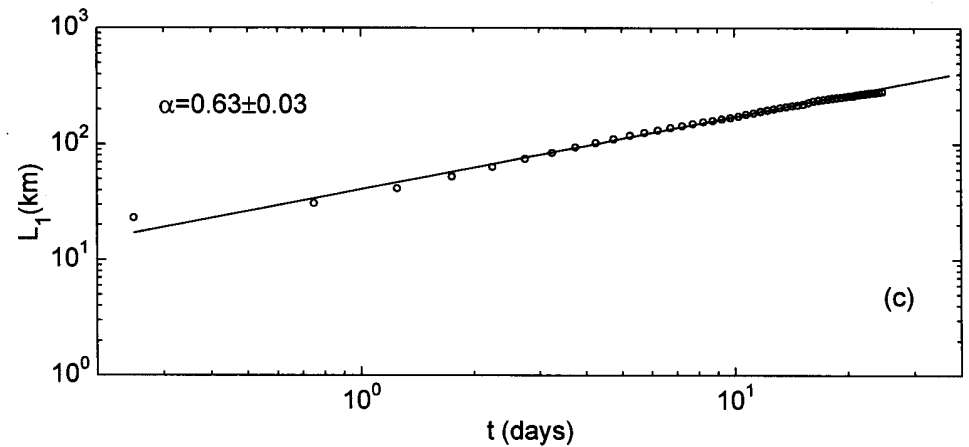
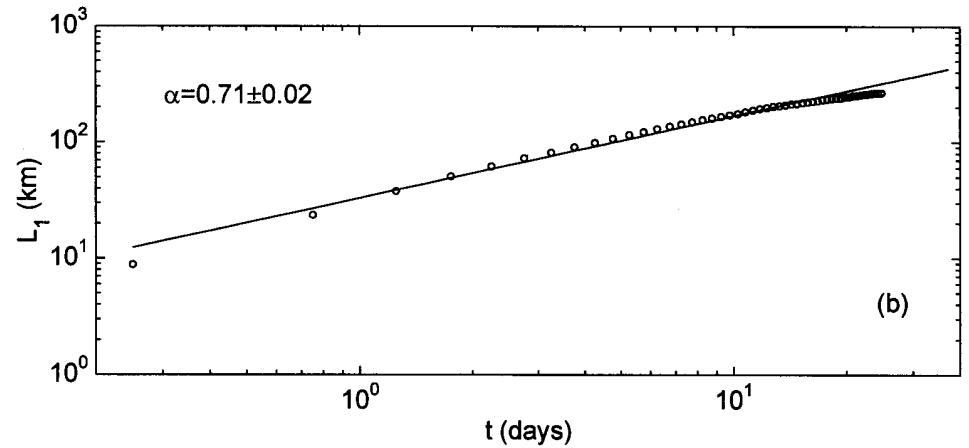
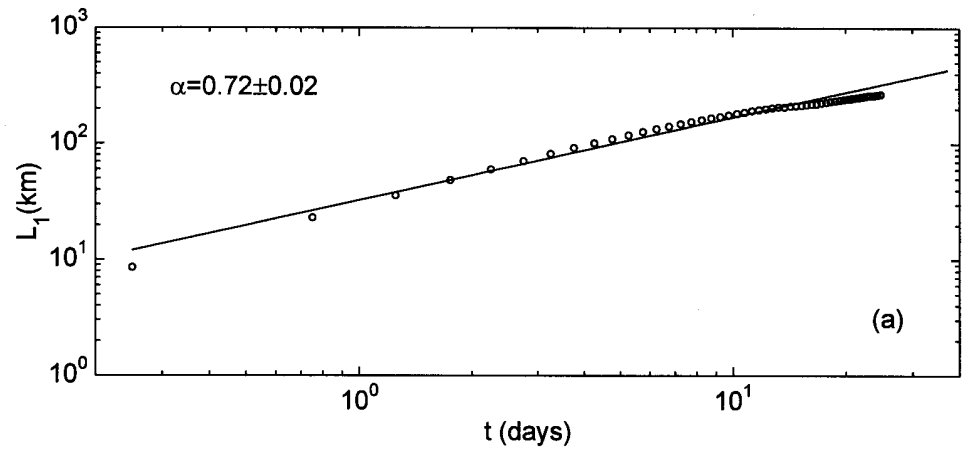


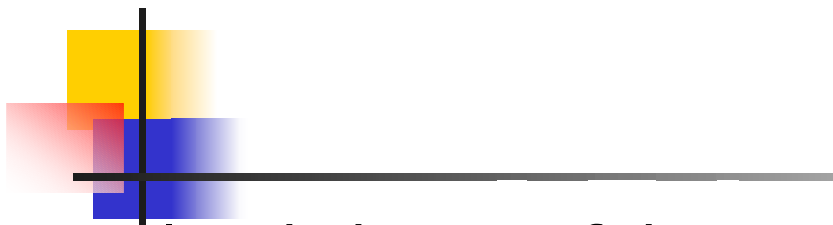
Scaling behavior of the
mean error (L_1) growth
for initial error levels:

(a) 0

(b) 2.2 km

(c) 22 km



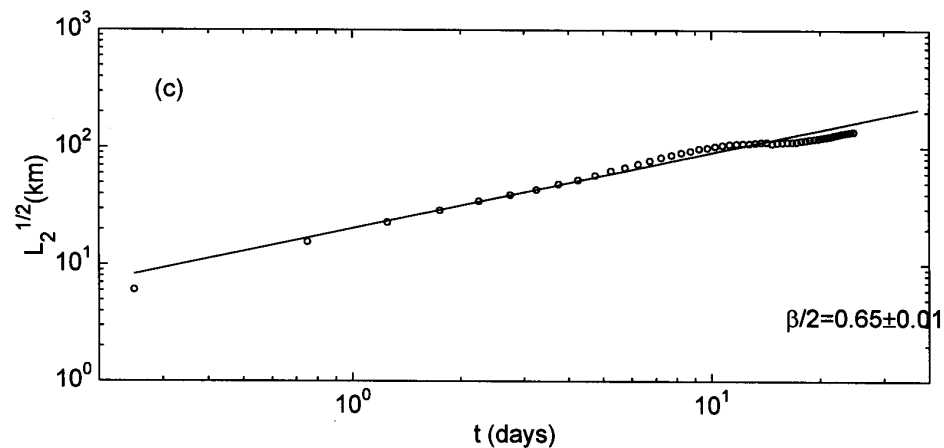
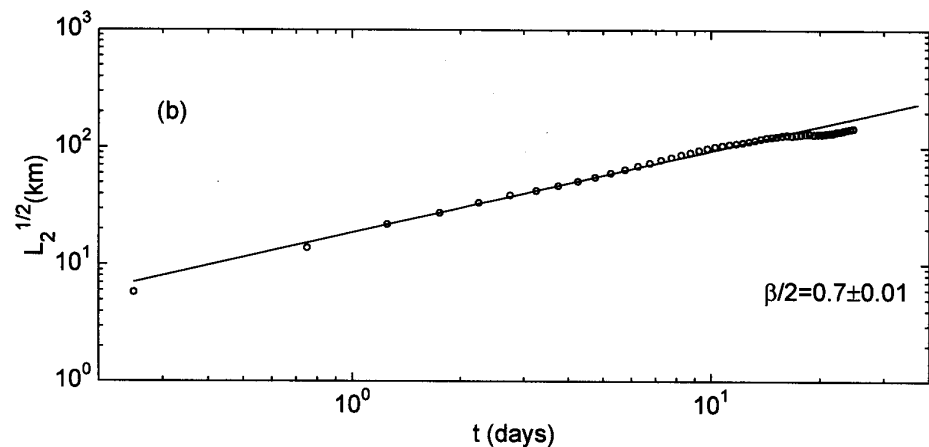
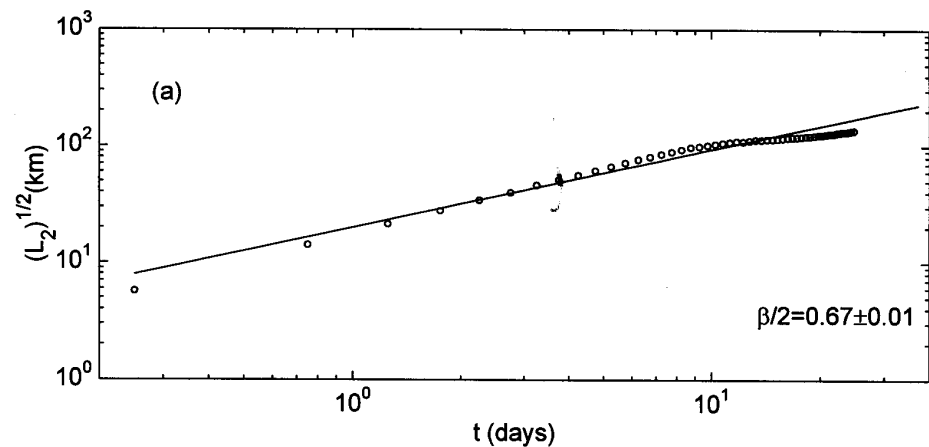


Scaling behavior of the
Error variance (L_2) growth
for initial error levels:

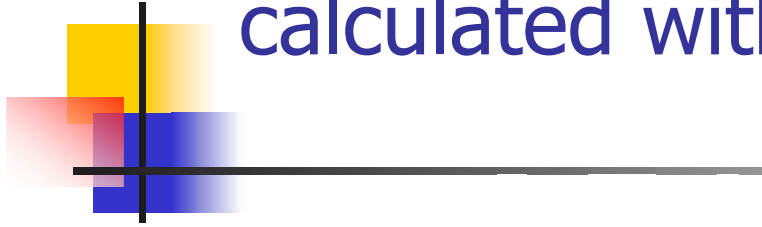
(a) 0

(b) 2.2 km

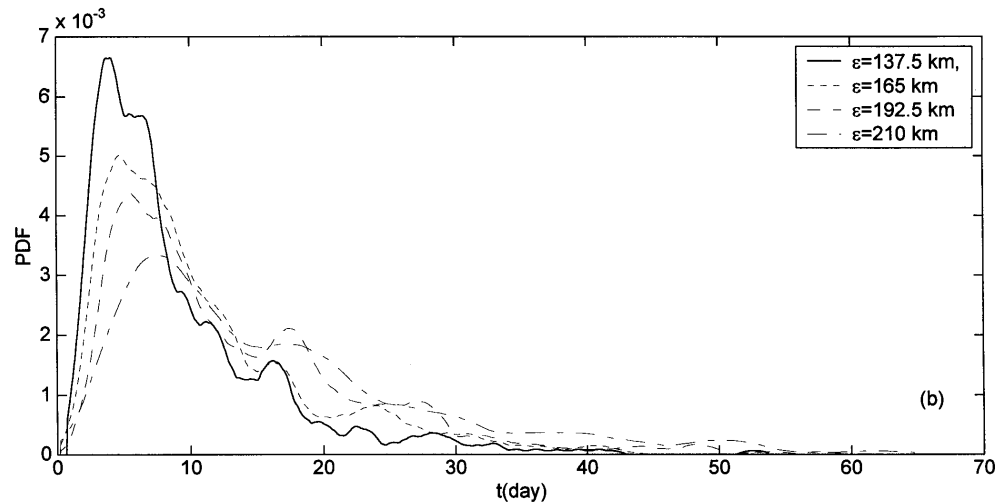
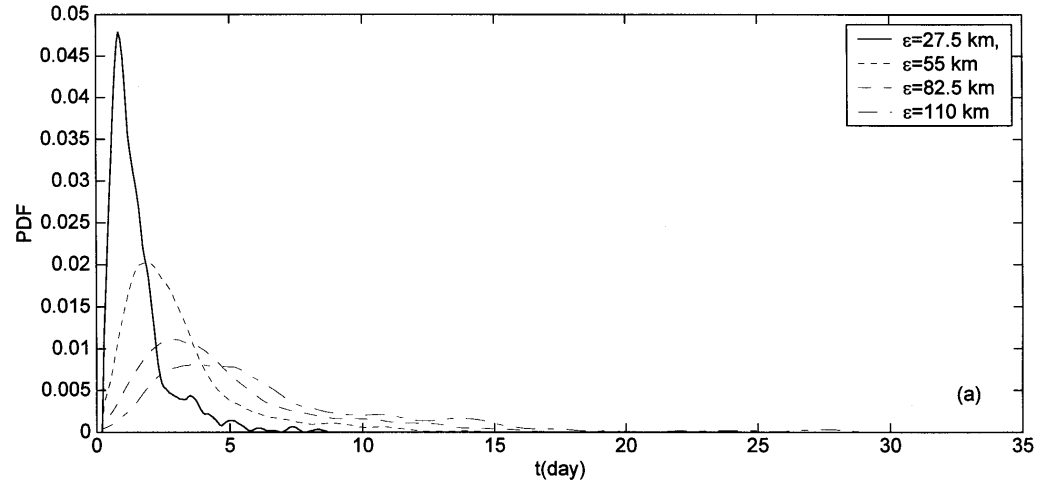
(c) 22 km

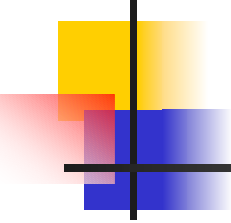


Probability Density Function of VPP calculated with different tolerance levels



Non-Gaussian distribution
with long tail toward large
values of VPP (Long-term
Predictability)





Conclusions

- (1) VPP is an effective prediction skill measure (scalar).
- (2) Backward Fokker-Planck equation is a useful tool for predictability study.
- (3) Stochastic-Dynamic Modeling